

POLITECNICO DI TORINO

Corso di Laurea Magistrale in Ingegneria Civile

Tesi di Laurea Magistrale

**EARTH, MOON, AND MARS: THE INFLUENCE OF  
THE ENVIRONMENT ON STRUCTURAL DESIGN  
AND CHOICE OF CONSTRUCTION MATERIALS**



Relatore:

Prof. Matteo Pavese

*firma del relatore*

.....

Candidato:

Ana Carolina Corrêa Caracas

*firma del candidato*

.....

Co-relatore:

Prof. Amedeo Domenico Bernardo Manuello Bertetto

*firma del co-relatore*

.....

A.A. 2022/23

# ABSTRACT

One of the primary goals of Space Exploration is the search for alternative living environments for humans, with the Moon as most feasible target and primary destination, and Mars as the subsequent central focus of attention, being one of the most Earth-like planets in the solar system. Overall, sustaining life beyond Earth is complex, but such pursuit of scientific knowledge and discovery can not only expand human presence across the Solar System but also address environmental issues on our home planet. As promising as the opportunities are in this field, there are significant challenges to overcome due to the markedly different environments outside the Earth, including varying atmosphere, gravity, surface characteristics, temperature fluctuations, and exposure to radiation and micrometeoroids. Therefore, before designing any space probe, vehicle, or structure, it is vital to understand how it fits into a mission and the requirements it must fulfil. The present work aims to contribute to the context of human extra-terrestrial settlement, with a focus on the influence of the terrestrial, lunar, and Martian environments on structural design and choice of construction materials. Building upon state-of-the-art contributions to space science and past unmanned satellite and rover missions, it is observed that the main loads acting on the structure are the self-weight in low gravity and the concomitant internal pressurisation of the habitat, applied to sustain human life. Using these conditions as a starting point, an optimized shape is proposed for each scenario using the Multi-Body Rope Approach (MRA), which is a form-finding iterative process based on the dynamic equilibrium of falling masses interconnected by a network of rope elements in the space-time domain. While on Earth structures must withstand gravity, the internal pressure of the lunar and Martian ones creates substantial loads, in an almost inverse analysis, which is illustrated by the MRA results. Following this, a discussion on construction materials is presented, with a focus on prioritizing the use of In-Situ Resources where possible. In conclusion, it's evident that the different conditions have a distinct impact on the shape and material composition of a structure, and understanding this influence is crucial when designing for the ever-evolving space industry.

**Keywords:** Moon, Mars, Structure, Form-finding, Materials, Comparative analysis.

# TABLE OF CONTENTS

<b>ABSTRACT .....</b>	<b>2</b>
<b>INTRODUCTION.....</b>	<b>6</b>
<b>CHAPTER 1: SPACE EXPLORATION AND THE STUDY OF DIFFERENT ENVIRONMENTS ..</b>	<b>9</b>
<b>CHAPTER 2: THE MULTI-BODY ROPE APPROACH.....</b>	<b>15</b>
2.1 THE MRA METHOD .....	15
2.2 MRA FOR SPACE APPLICATION .....	21
<b>CHAPTER 3: ANALYSIS FOR LUNAR AND MARTIAN ENVIRONMENTS .....</b>	<b>29</b>
3.1 TYPES OF STRUCTURES.....	29
3.2 STRUCTURE PROPOSITION .....	35
<b>CONCLUSION .....</b>	<b>43</b>
<b>REFERENCES .....</b>	<b>44</b>

## LIST OF FIGURES

Figure 2.1: Initial grid (MATLAB ©).....	16
Figure 2.2: Representation of node “i”, connected to four other nodes.....	17
Figure 2.3: Funicular shape obtained for the 10x10 grid (MATLAB ©).....	20
Figure 2.4: Modified representation of node “i”.....	21
Figure 2.5: projected areas for node “i”.....	22
Figure 2.6: 25-node grids on each of the three environments .....	23
Figure 3.1: Class I, II and III habitats.....	30
Figure 3.2: Lunar pits (based on LROC).....	31

## LIST OF TABLES

Table 1.1 Comparable data from the Earth, Moon, and Mars.....	12
Table 2.1 Types of nodes and respective degrees of constraint.....	19
Table 2.2: Different node grids on each of the three environments .....	24
Table 2.3: Impact of different nodal masses.....	26
Table 2.4: Impact of different maximum lengths.....	27
Table 2.5: Changes in maximum lengths for a 5x5 grid.....	28
Table 3.1: Lunar pits (based on LROC).....	32

# INTRODUCTION

The subject of space has always captivated human interest, from ancient studies of the night sky to the first geared mechanical astrolabe in the 1200s and Galileo Galilei's astronomical observations in the 1600s. With advancing technology, there is an expected growth in both curiosity and the possibilities for exploration in this captivating domain. What was before only observable with telescopes and other low-cost tools, became a reality for astronauts crossing the boundaries of Earth's atmosphere. Another example is found in the historical evolution of rocket science, extending back over a millennium, with the use of fire arrows propelled by gunpowder in China. This expertise was further enhanced as it spread to other parts of Asia and Europe, reaching Islamic Spain by the mid-1200s. Nowadays, state-of-the-art rockets allow the exploration of planets, moons, and comets in the farthest reaches of our Solar System. Similarly, the desire to establish human colonies outside of the Earth is not exclusive to our current generations. Works of the writers Cyrano de Bergerac (1687), Samuel Brunt (1727) and Jules Verne (1865) have imagined crewed voyages to the Moon even before the launch of the first artificial satellite. Since then, exploration of deep space has seen decades of technological advancement and scientific discoveries, making what was fiction now a booming industry. [1]

Currently, the most prominent plan to establish human colonies on the Moon and Mars is the Artemis initiative, an international program led by the National Aeronautics and Space Administration (NASA). Named after the Greek goddess and twin sister of Apollo, the program is divided in three phases and aims at taking humanity back to the Moon. Advancing in complexity, the phases go from flight tests in lunar orbit in Artemis I, to sending a crewed flight to the lunar environment for the first time in over 50 years in Artemis II, and finally a new Moon landing in Artemis III, including the first woman to walk on its surface. After Artemis III, missions on and around the Moon will lay the foundation for a human journey to Mars – and beyond. The creation of this program, as well as proposals by Elon Musk's SpaceX and Jeff Bezos' Blue Origin, are testament to the relevance of the topic not only under the public eye, but also for private and public institutions. The natural satellite's proximity to our planet makes it a more feasible target for establishing a sustainable human presence, but it is most certainly not the sole destination, but a stepping stone for human exploration of deep space. In this context, Mars is the succeeding central focus of attention in the search for alternative living environments for humans, as one of the most Earth-like planets in the solar system. [2, 3]

NASA's plans for human space exploration are ambitious, and international collaboration is key to achieve its milestones that culminate on the founding of a sustainable human presence on the Moon, followed by human missions to Mars and other deep-space destinations. This long-term goal is significantly different from the current state of exploration missions, which are mostly performed by unmanned rovers and probes, such as Mars 2020 Perseverance rover and Ingenuity unmanned aerial vehicle (UAV). Manned missions, although present on the Moon between 1969 – when Neil Armstrong started the first moon landing – and 1972 – the last manned mission to the Moon, with Apollo 17 – are so far only short-term. This paradigm shift, from conducting either transitory or robotic missions, to founding human settlements and mining operations, is associated with various challenges, including the long duration of the journey, the need for radiation protection, and the development of advanced life support systems and habitats. To address such issues, state-of-the-art technologies on deep space habitation, spaceflight, and landing capabilities are being developed with the help of long-standing International Space Station partners such as the European Space Agency (ESA) and the Japan Aerospace Exploration Agency (JAXA). Having multidisciplinary and international collaboration as pillars is not an exclusive trait of this new generation of space missions. For nearly 25 years, hundreds of astronauts from over 20 countries have lived and worked aboard the International Space Station (ISS) 250 miles above Earth. [2, 4]

In a simplistic manner, sending humans outside the Earth and the strategies and technologies being developed to support such task can be divided into two steps: launching and settlement. Currently, some important players tackling the first point are the Space Launch System (SLS) rocket and the Orion spacecraft. Respectively, they are the most powerful rocket ever built and the vehicle designed to transport astronauts beyond low-Earth orbit, enduring the harsh conditions of deep space and powered by a service module provided by ESA. [2] The second part of the mission – settling on the Moon, and later Mars – comprehends a complex and multidisciplinary subject, to which the topic proposed on this thesis aims at contributing, with a focus on the influence of the environment on structural design and choice of construction materials. Building upon state-of-the-art contributions to space science, this work analyses the impact of low-gravity and the concomitant pressurisation of the habitat (to sustain human life) on the optimised shape of the same structure on lunar and Martian environment with comparison to the Earth.

An initial analysis is done by using the Multi-Body Rope Approach (MRA), a form-finding technique used to obtain the optimised shape of complex shell and gridshell structures. This already provides a few insights on the behaviour of the spatial habitat

in comparison to a terrestrial one. Moreover, the different habitat construction possibilities and material applications are indicated, followed by the strategy chosen for this work. In the sequence, the structure is analysed using the Finite Element Analysis (FEA) software LUSAS ©, as the MRA approach defines the geometry of the problem but not the internal stresses.

Before achieving the end-goal, important information shall be presented on both Planets and the Natural Satellite, as well as on the context of Space Exploration. Understanding of the history of Space exploration, its challenges, and opportunities, as well as the requirements unique to such harsh environments is essential to dimensioning any space structure. Key information on the topic, as well as a comparison between the two alternative environments and that found on our planet are presented in the sequence.



# CHAPTER 1: SPACE EXPLORATION AND THE STUDY OF DIFFERENT ENVIRONMENTS

As previously stated, the study of the Solar System has fascinated scholars and enthusiasts for millennia, but it was between the decades of 1950 and 1970 that it became a topic of interest for whole nations. In 1957, Soviets began to accomplish a series of milestones in space exploration with the launch of Sputnik 1, the first artificial satellite, and later the first earthling in orbit – a Russian dog named Laika. Additional leading-edge accomplishments by the Soviet Union include the first man – Gagarin, and later the first woman – Tereshkova, launched into outer space, as well as the first spacewalk, the first spacecraft to orbit the Moon, and the first unmanned spacecraft to land on the lunar surface. Broadcasted internationally, the aerospace accomplishments marked a generation, culminating in Armstrong's first steps on the Moon in 1969. In 1975, a joint US and Soviet space mission named Apollo-Soyuz was successfully staged in low-Earth orbit. The two spacecraft docked and the commanders Stafford and Leonov greeted each other with an official handshake in space, marking it the first international space collaboration. [2]

The launch of Sputnik 1 kicked-off a new era of knowledge, with the first Russian and American imaging missions between 1959 and 1965. Simultaneously, an earth-based mapping on the Moon by telescope led to the determination of its stratigraphy. The information on the natural satellite was later complemented by the first orbital gamma-ray chemical data and the first soil physics and chemistry data collected by unmanned rovers and transmitted by radio (1966). In the 1970's, the first samples were taken by Soviet Luna robots and crew from six Apollo landings. Although the Moon was the only destination explored by astronauts, Mars is the most widely investigated planet in the solar system. Even before the remarkable human landing in 1969, the neighbour planet was already valued as a topic of research. NASA's Mariner 4 (1965) is considered the first successful mission to Mars for flying by the planet and capturing the first close-up images of its surface. Certainly, these studies have been greatly facilitated with the advancement of technology. A valuable example is the contribution of Mariner 9, the first spacecraft to orbit another planet (Mars). Before 1971, there was a false impression that the planet's surface looked like the Moon because the first crafts to capture images from Mars (Mariner 4, Mariner 6, and Mariner 7) happened all to fly over areas that were covered in craters. This was refuted by the discoveries of the orbiter and the understanding that what seemed to be craters were actually the tops of dormant volcanoes. [5, 6]

Since the first closer contact in 1965, the quantity and level of detail of the information available on the planet has risen significantly. Particularly, nearly thirty missions from different space agencies have successfully explored the Red Planet with different types of probes. Present missions aim to study the geology and potential habitability of Mars and search for signs of microbial life, in particular looking for traces of ancient water. The major role of this element for sustaining life can be understood with an investigation on our own planet's history, as explained by the Adler Planetarium:

“According to evidence from radiometric dating and other sources, Earth was formed about 4.54 billion years ago. Within its first billion years, life appeared in its oceans and began to affect its atmosphere and surface, promoting the proliferation of aerobic as well as anaerobic organisms and causing the formation of the atmosphere's ozone layer. This layer and the geomagnetic field blocked the most life-threatening parts of the Sun's radiation, so life was able to flourish on land as well as in water. Since then, the combination of Earth's distance from the Sun, its physical properties and its geological history have allowed life to thrive and evolve.”

Considering such importance, scientists were enticed by the detection of the first ancient signs of water in Mars, such as gullies formed by moving liquid and hematite (a mineral that forms in water), revealed by Mars Global Surveyor (1997), and further investigated by the twin rovers Spirit and Opportunity (2004). Curiosity (2012), presently operational and equipped with an on-board laboratory, landed in Mount Sharp within Gale Crater, and discovered signs of an ancient streambed, ancient sands carried by water and key chemical ingredients for life, as well as clay minerals formed in water. These major findings reveal that, long ago, this crater was habitable and contained streams, ponds and even mud. Likewise, Perseverance found evidence that rocks in Jezero Crater interacted with liquid water long ago. It purposely landed near an ancient river delta, searching for deposits of clay and carbonate – minerals that only form in the presence of water. Features and rock layers on the surface shaped by water indicate that the temperature and pressure were higher in the past. Thus, although in the present Mars is cold and mostly dry, it was once a warmer and wetter world. If determined that even microbial life ever existed on Mars, and whether it would survive there today, it could be concluded that life may be fairly commonplace in the Universe. [6]

The presence of water ice has also been confirmed on the Moon. Permanently shadowed regions near the lunar poles intrigued scholars since the first detailed mapping of the Moon in 1994, and the Lunar Prospector mission (1998-1999) suggested the presence of hydrogen by measuring the flux of neutrons on its surface.

In the following decade, the Indian Chandrayaan-1 detected hydroxyl (OH) and water in the lunar soil, confirming the presence of water molecules. Since then, other missions also identified water vapor in the lunar regolith and mapped hydrogen distribution, representing potential water ice deposits. The most promising location for a crewed lunar mission is the South Pole, near the Shackleton crater, chosen as landing point for the future Artemis Base Camp. Benefits of this area are not limited to the location of water ice, but also a constant view of the Earth – primordial for the psychological health of the crew. [2, 7]

Given the relevance and excitement in such findings, numerous missions oversee exploring places in our Solar System too distant, dangerous, or expensive for humans to visit. In addition to preparing for extra-terrestrial living, studying another planetary bodies provides insight into Earth's formation and history in the same way that our detailed knowledge about our planet helps us understand other bodies in the Solar System – this is called comparative planetology. The understanding of a different ecosystem, and development of the necessary technologies and infrastructure for human missions are advantageous for several fields of knowledge. Besides understanding the origin and distribution of life in the universe, advancements in the fields of engineering, robotics, and natural sciences can have applications beyond space exploration, such as in renewable energy, environmental monitoring, and disaster response, as well as providing opportunities for education and public engagement in science. [6]

Discoveries like this motivate the scientific community to prepare for future human settlements on the Moon and Mars, such as the topic of this work. As coined by the Artemis plan, “the Moon is the gateway to the solar system”, expanding from robotic to crewed missions. The clearest advantage is the distance, with a journey of about 3 days, while to reach Mars would take several months. This closeness guarantees the feasibility of the trip, already proved possible in the last decade, and encourages teleoperating, with a radio delay within seconds. On the other hand, technology for a longer, more expensive trip to Mars is not available yet to ensure the comfort and safety of the crew. However, the selection of Mars as the second target is not arbitrary. Of all the other planets in our Solar System, this one has the most Earth-like conditions and plentiful water, although most of it is now frozen below the surface or in the polar caps. The period of revolution and the inclination of the axis are also close to what is observed on Earth, implying a comparable alternation of seasons and day-night cycle. This poses an advantage for the psychological well-being of the crew. [8, 9]

Despite the similarities, there are key differences to be considered, such as the Moon's practically inexistent and Mars' thin atmosphere, leaving the crew vulnerable to cosmic radiation. Daily temperature variation is also higher than on Earth, and the differences in size and volume are also significant, as they result in reduced gravity. For this and other characteristics, they are considered extreme environments and missions must be planned accordingly. Table 1.1 contains an initial comparison between the three environments, which will be complemented in succeeding chapters as more detailed data is required for the habitats dimensioning.

Table 1.1: Comparable data from the Earth, Moon, and Mars [6, 10]

	Earth	Moon	Mars
General information	<ul style="list-style-type: none"> <li>– Third planet from the Sun, the densest planet in the Solar System, and the largest of the four terrestrial planets</li> <li>– Has one rounded moon</li> </ul>	<ul style="list-style-type: none"> <li>– Earth's solitary satellite</li> <li>– Average distance from the Earth: 378000 km</li> </ul>	<ul style="list-style-type: none"> <li>– Fourth planet from the Sun; has two potato-shaped, small moons</li> <li>– Average distance from the Earth: 56-149 Mio. km</li> </ul>
Planetary information	<ul style="list-style-type: none"> <li>– Length of day = 24 hours</li> <li>– Orbit: 1 year = 365,2 days</li> <li>– Mass: <math>5.97 \cdot 10^{24}</math> kg</li> <li>– Equatorial diameter: 12756 km</li> <li>– Gravity: <math>g = 9.81 \text{ m/s}^2</math></li> </ul>	<ul style="list-style-type: none"> <li>– Length of day = 708.7 hours</li> <li>– Orbit: 27.3 days (around the Earth) – half of this time it is completely dark, except on the poles</li> <li>– Mass: <math>7.35 \cdot 10^{22}</math> kg = 0.0123 Earths</li> <li>– Equatorial diameter: 3475 km = 0.27 Earths</li> <li>– Gravity: 0.17 g = <math>1.62 \text{ m/s}^2</math></li> </ul>	<ul style="list-style-type: none"> <li>– Length of day = 24.7 hours</li> <li>– Orbit: 1 year = 687 days = 1.88 Earth years</li> <li>Daylight distribution is similar to that on Earth</li> <li>– Mass: <math>6.42 \cdot 10^{23}</math> kg = 0.11 Earths</li> <li>– Equatorial diameter: 6792 km = 0.53 Earths</li> <li>– Gravity: 0.38 g = <math>3.73 \text{ m/s}^2</math></li> </ul>
Environmental information	<ul style="list-style-type: none"> <li>– Mean temperature: 15 °C</li> <li>– Temperature range: - 88 °C to + 58 °C</li> <li>– Average atmospheric pressure: 1 bar</li> </ul>	<ul style="list-style-type: none"> <li>– Mean temperature: - 20 °C</li> <li>– Temperature range: - 178°C to + 117°C</li> <li>Average atmospheric pressure: <math>3 \cdot 10^{-15}</math> bar</li> </ul>	<ul style="list-style-type: none"> <li>– Mean temperature: - 65 °C</li> <li>– Temperature range: - 89 °C to - 31 °C</li> <li>– Average atmospheric pressure: 0.01 bar</li> </ul>

	– Atmospheric composition: 78% nitrogen, 21% oxygen, 1% others	– Composition of the tenuous lunar atmosphere is poorly known	– Atmospheric composition: 95% carbon dioxide, 2.6% nitrogen, 2% argon, 0.16% oxygen, and others
Mission information		<ul style="list-style-type: none"> <li>– One-way trip in a rocket: 3 days</li> <li>– Mission duration: 6 to 12 months</li> <li>– Crew size: up to 4 astronauts</li> <li>– Communication delay: around 2 seconds</li> </ul>	<ul style="list-style-type: none"> <li>– One-way trip in a rocket: 6 months</li> <li>– Mission duration: &gt; 12 months</li> <li>– Crew size: up to 6 astronauts</li> <li>– Communication delay: between 4 and 24 minutes</li> </ul>

An initial comparison can grant some advantages to the Moon, mostly related to practicalities of the mission, and some to Mars, particularly in terms of similarities to the Earth. One advantage of the Moon is the constant, predictable and inexhaustible source of sunlight in the South Pole, which can be converted into electric power by solar panels. Moreover, closeness to the Earth permits continuous communication and monitoring, which would be very constrained in a Mars mission. Due to the larger distance, the degree of isolation can be considered as more critical on Mars, as well as the complications in case of an emergency. Lastly, Earth is only visible from the Moon, which can impact the psychological wellness of the astronauts. On the other hand, Mars has a more Earth-like day and night cycle and more tolerable temperature variations. While the Moon has little to no atmosphere, Mars' thin atmosphere provides some protection from solar particles and cosmic radiation, and is consisted mostly of carbon dioxide, which is good for plant life. A downside of the light atmosphere is the creation of wind and weather which, while balances the temperature variation, causes dust storms, something that is not present on the Moon. The so-called dust devils form when the Sun heats the ground to a warmer temperature than the atmosphere above it, causing warm air to rise in whirlwinds and pick up sand and dust, forming swirling columns up to 20 km high, at speeds of up to 100 km/h. Due to the low atmospheric pressure, the main effect of such storms in a structure would not be due to wind power, rather the degradation of exposed surfaces. They are also highly predictable, and astronauts can take cover and harness the wind for energy. [8]

Upon first assessment, Martian environment seems more friendly to astronauts, but the obstacle of distance cannot be overlooked. Due to the large distance from the

Earth, a trip to Mars would have a duration of approximately 6 months with the present spaceship technology, departing when the two planets are closest together with an aligned orbit. Once the crew arrives, estimated stay is of approximately one year before initiating the return home, with a total mission duration of circa 2 years. Differently than current missions to the ISS, or former Apollo missions to the Moon, it is physically and financially demanding to perform round trips to Mars, with the astronauts spending months to arrive and only a few hours on the planet, as current spacesuits allow for a maximum of 8 hours of space exploration time. Consequently, the success of human missions on the Red Planet relies on the construction of a shelter, fully habitable and protected from the extreme environment, as well as adequate rocketry for a longer mission. For this and other reasons, NASA's Artemis plan aims at establishing a lunar presence before attempting trips to Mars. With the close distance and the discovery of water ice in the polar regions, it is considered the best target for now. Building upon the progress and experience gained from previous missions to the Moon and low-Earth orbit, as well as future advancements during the first phases of Artemis, the technology required for the construction of surface habitats is projected to be evolutionary in nature. [2, 8]

Due to the novelty and ever-changing nature of the subject, the Technology Readiness Level is still quite low, a level 2 – technology concept and/or application formulated. Therefore, the proposed solutions are based on fundamental principles and are expected to be improved with the advance of scientific knowledge and state-of-the-art technologies. Moreover, there is an issue of industry secrecy and competition. With various players exploring the same topic, it is likely that questions arising for one team could be answered by the findings of others, highlighting the importance of international collaboration. On the other hand, studying a topic of low TRL presents the opportunity to contribute to a time of paradigm shift, aiming to allow manned long-term missions outside of the Earth instead of only robotic or short-term ones, as is the current norm. Many are the challenges to be overcome before Artemis III, when surface habitats, together with pressurised and unpressurised rovers will enable long-duration crewed missions, but the available knowledge already provides interesting insights. One of the fundamentals of space design is the minimization of structure mass due to restrictions on rocket payloads. Likewise, structural design shall aim for simple load paths while withstanding applied loads due to the natural and induced environments to which they are exposed during the service life. Aiming at optimising the shape of a structure on lunar and Martian environment, subjected concomitantly to the reduced gravities of each system and an internal pressurisation to host human life, the chosen method is the Multi-Body Rope Approach, to be discussed in the subsequent chapter. [11, 12]

## CHAPTER 2: THE MULTI-BODY ROPE APPROACH

The Multi-Body Rope (MRA) approach is a form-finding method that can be applied to determine the optimised shape of a grid shell structure. Firstly, it is possible to define grid shell as a structure with a single thin layer and a thickness very small in comparison to the main span to be overcome. Defined by the interaction between their shape and stress distribution, it is ineffective to design them in the conventional way. Secondly, form-finding is a process to determine the geometry configuration of a structure in order to obtain minimal internal stresses for a certain loading arrangement. There are several other approaches, physical and mathematical, to obtain such optimised shape, as well as solutions generated by computer aided design software. A noticeable example of form-finding application is the hanging model of Gaudí, author of La Sagrada Familia and Casa Milà in Barcelona. However, not every commercially available structural analysis software is suited for analysing grid shell structures, particularly for very large displacements. As a solution, Italian scholars Bertetto, Melchiorre, Sardone and Marano, from Politecnico di Torino and Politecnico di Bari, developed a MATLAB © code for shape optimisation of grid shells. [13]

### 2.1 THE MRA METHOD

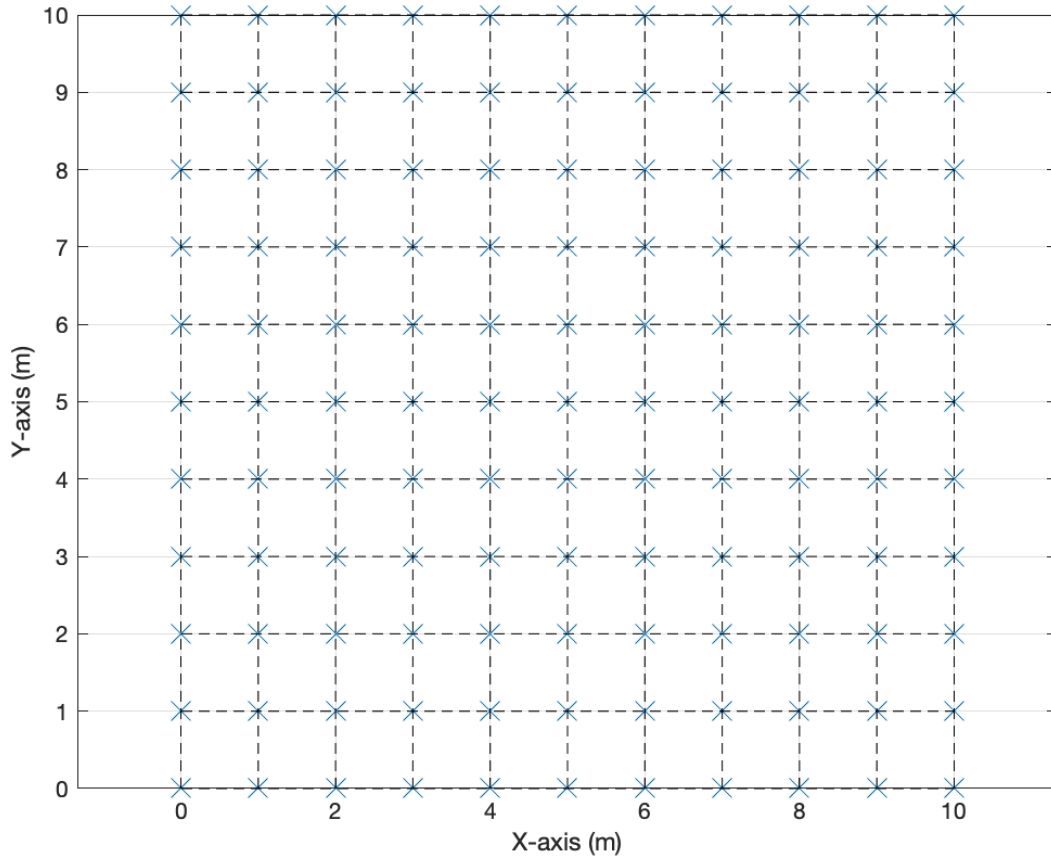
The method leverages a self-made code based on the dynamic equilibrium, ensured by the d'Alembert principle, of a hanging grid formed by free masses connected by flexible rope elements in the space-time domain. The main characteristic that distinguishes this model is the use of real ropes to simulate the suspended shape created by the hanging net, while in other models the self-weight of the nodes and the load of the rods are focused on the nodes. Therefore, there is a difference on the system of forces acting on the nodes. In this way, the rope is not stressed when the distance between endpoints on the final configuration ( $l_i$ ) is smaller than that of the initial one ( $l_f$ ) – the prefixed rope length. When these are equal, forces of equal magnitude and opposite direction are applied at the endpoints and no bending is observed (except due to limitation in any of the degrees of freedom). The ropes behave, thus, in full traction.

$$F = \begin{cases} 0 & , l_i < l < l_i \\ F_{max} & , l \geq l_f \end{cases} \quad (\text{Equation 2.1})$$

Once every input information is defined, the iterative process of falling masses can be computed. To obtain its static configuration, a set of equilibrium equations are solved in the time domain. Step-by-step, the corresponding node coordinates can be calculated by the different velocity and acceleration of the falling masses (nodes) with respect to the previous step. Numerically, the hanging of the net is simulated by the dynamic equilibrium with inertial actions until achieving the final equilibrium configuration, corresponding to the conditions of zero velocities and zero accelerations of the nodes. The optimized shape can be represented by the upturned model consistent to the final step of this iterative analysis. The obtained funicular form is the 3D equivalent of a catenary, solely under axial loads, minimising the bending moment. [13, 14]

To illustrate the method and its application, consider a squared grid with quadrilateral mesh, dimensions 11 x 11 nodes and unitary spacing, illustrated in Figure 2.1. If representing a roof, for example, the span would be of 10 x 10 meters.

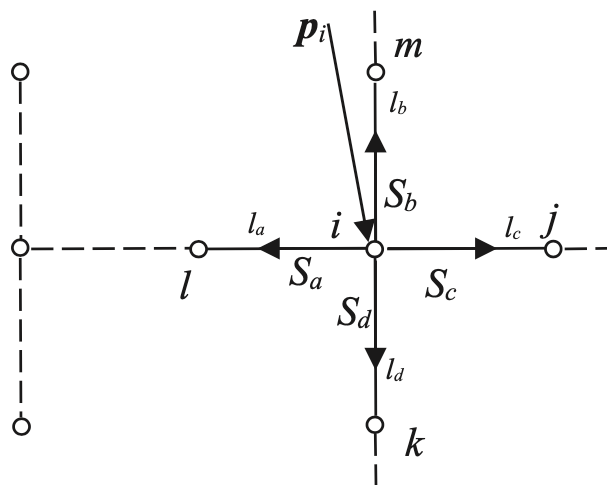
Figure 2.1: Initial grid (MATLAB ©)





As mentioned previously, an intrinsic characteristic of this method is the system of forces acting on the node. Thus, taking a generic node “i” of this grid, of coordinates  $x_i, y_i, z_i$ , connected to four other nodes ( $j, k, l, m$ ) and, consequently, four rope elements ( $a, b, c, d$ ), at least five loads are acting on the node “i”: the forces relative to each rope element and the external ones. In this example the structure is considered subjected to only self-weight, due to gravity on Earth, and the fifth force is represented by the letter p, as illustrated below.

Figure 2.2: Representation of node “i”, connected to four other nodes [14]



The equilibrium of the node can be represented as:

$$\vec{R}_i = \vec{p}_i + \vec{s}_a + \vec{s}_b + \vec{s}_c + \vec{s}_d + \vec{F}^I + \vec{F}^{II} = 0 \quad (\text{Equation 2.2})$$

where

$\vec{R}_i$  is the resultant in the node “i”,

$\vec{F}^I$  is the inertial force, of module  $F = m \cdot a$  – the product between the mass of the node and the amplitude of the acceleration vector – and opposite direction to the acceleration,

$\vec{F}^{II}$  is the dissipative force, equal to the product of a constant times the velocity vector, and opposite direction to the velocity, and

$\vec{s}_a, \vec{s}_b, \vec{s}_c, \vec{s}_d$  represent the resultants along the rope elements  $a, b, c, d$  and  $\vec{p}_i$  the external forces applied to the node "i".

Starting from the plane configuration of the grid and the applied forces just explained, the next-step configuration can be obtained with the dynamic balance equations, as represented in equations 2.4 to 2.6, based on the principles of dynamics [15] and the node configuration of Figure 2.3.

$$m\ddot{x}(t) + c\dot{x}(t) + kx(t) = F(t) \quad (\text{Equation 2.3})$$

$$\frac{x_i - x_j}{l_a} S_a + \frac{x_i - x_k}{l_b} S_b + \frac{x_i - x_l}{l_c} S_c + \frac{x_i - x_m}{l_d} S_d + p_{ix} - m_i \ddot{x}_i - c_i \dot{x}_i = 0 \quad (\text{Equation 2.4})$$

$$\frac{y_i - y_j}{l_a} S_a + \frac{y_i - y_k}{l_b} S_b + \frac{y_i - y_l}{l_c} S_c + \frac{y_i - y_m}{l_d} S_d + p_{iy} - m_i \ddot{y}_i - c_i \dot{y}_i = 0 \quad (\text{Equation 2.5})$$

$$\frac{z_i - z_j}{l_a} S_a + \frac{z_i - z_k}{l_b} S_b + \frac{z_i - z_l}{l_c} S_c + \frac{z_i - z_m}{l_d} S_d + p_{iz} - m_i \ddot{z}_i - c_i \dot{z}_i = 0 \quad (\text{Equation 2.6})$$

The contribution of the velocity and the acceleration for each node, as well as the length of the rope elements can be expressed as:

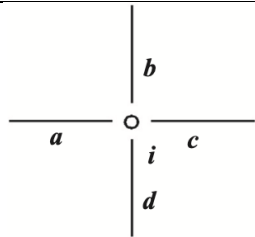
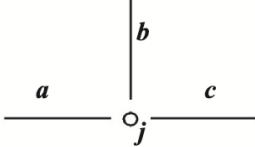
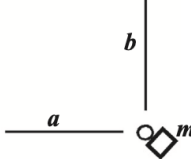
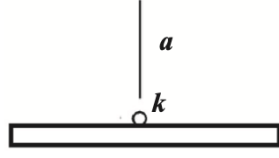
$$\dot{x}_i = \frac{\partial x_i}{\partial t} \quad \dot{y}_i = \frac{\partial y_i}{\partial t} \quad \dot{z}_i = \frac{\partial z_i}{\partial t} \quad (\text{Equation 2.7})$$

$$\ddot{x}_i = \frac{\partial^2 x_i}{\partial t^2} \quad \ddot{y}_i = \frac{\partial^2 y_i}{\partial t^2} \quad \ddot{z}_i = \frac{\partial^2 z_i}{\partial t^2} \quad (\text{Equation 2.8})$$

$$l_{rope} = \sqrt{(x_i - x_j)^2 + (y_i - y_j)^2 + (z_i - z_j)^2} \quad (\text{Equation 2.9})$$

To ensure the dynamic falling of the net, an appropriate number of degrees of freedom must be defined, which depends on the constraint system. For the correct level of hypostatic condition, the number of degrees of freedom (D.o.F.) must be higher than the degree of constraint of the three-dimensional system (D.o.C.). The latter depends on the typology of the node, as broken down in the following table:

Table 2.1: Types of nodes and respective degrees of constraint

	Node typology	Number of adjacent nodes	D.o.C.
A		4	9
B		3	6
C		2	6
D		1	3

The total number of degrees of constraint and degrees of freedom of the system can be calculated as:

$$D.o.C. = n_A \cdot 9 + n_B \cdot 6 + n_C \cdot 6 + n_D \cdot 3 + n_t \cdot 1 \quad (\text{Equation 2.10})$$

$$D.o.F. = n_t \cdot 6$$

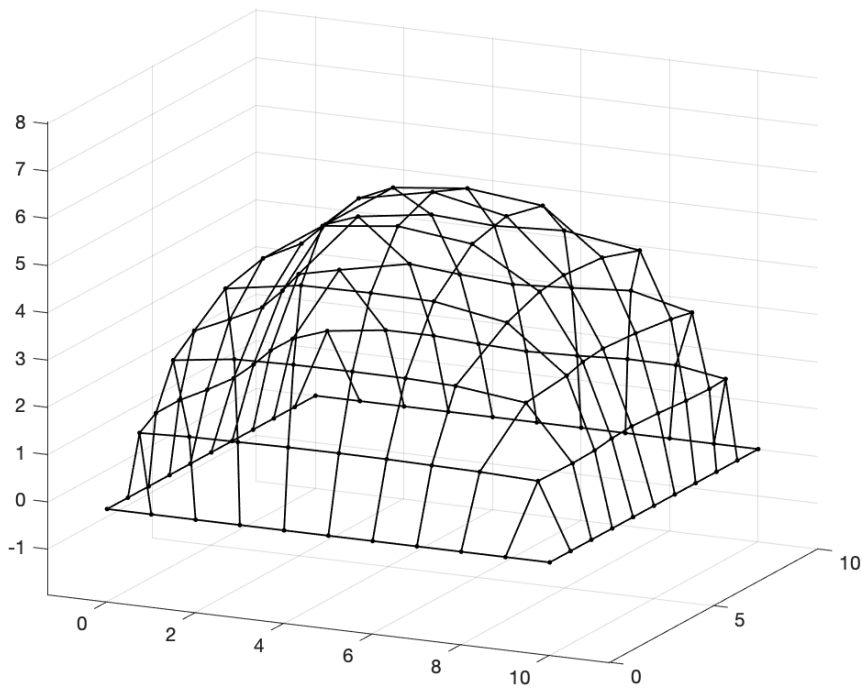
where:

$n_A, n_B, n_C, n_D$  are the number of nodes corresponding to the situations A, B, C or D presented in Table 2.1.

$n_t$  is the number of nodes. [13, 14]

The result of form-finding leads to the shell structure illustrated in Figure 2.3.

Figure 2.3: Funicular shape obtained for the 10x10 grid (MATLAB ©)



In this framework, the geometry can be subjected to any kind of load, such as wind pressure and self-weight, as long as it can be characterized by a group of constants in x,y,z directions. E.g., self-weight of the structure due to gravity on Earth can be represented by the vector:

$$[0 \ 0 \ 9.81 \cdot m]$$

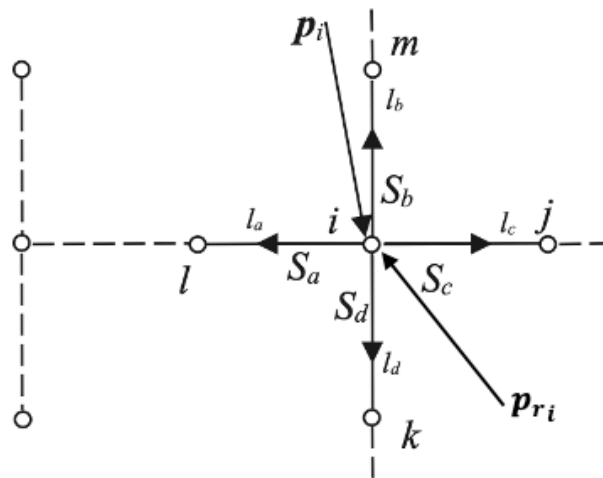
In which  $m$  is the mass of each node in kg.

While this representation works for the loading conditions of most structures on Earth, design for space has a key feature: internal pressure, which must be accounted for in its correct intensity and direction, both depending on the geometry. To correctly represent this additional force, a few modifications were done to the MRA code, as follows.

## 2.2 MRA FOR SPACE APPLICATION

Besides considerations on temperature variation, cosmic radiation, or different soil composition, the main factor that differs a structure on Earth to that on the Moon and Mars is the internal pressurisation, essential to sustain life. As commented previously, whereas on Earth the average atmospheric pressure is of 101.3 kPa, on Mars it is much lower, with an average of 610 Pa, and on the Moon, it is practically inexistent, so that it can be considered as embedded in hard vacuum. To account for this pressure and its correct direction, the original MRA code was modified to include a force that depends on the area of application. Differently than constant loads, the vector correspondent to pressure, applied to each node, changes at each time step, both in intensity and direction, as the geometric configuration follows the falling masses trajectory. Therefore, a modified representation of the node “i” can be shown:

Figure 2.4: Modified representation of node “i”



The equilibrium of the node can be represented as:

$$\vec{R}_i = \vec{p}_{ri} + \vec{p}_i + \vec{s}_a + \vec{s}_b + \vec{s}_c + \vec{s}_d + \vec{F}^I + \vec{F}^{II} = 0 \quad (\text{Equation 2.11})$$

where

$\vec{R}_i, \vec{F}^I, \vec{F}^{II}, \vec{s}_a, \vec{s}_b, \vec{s}_c, \vec{s}_d$  represent the same vectors as in Equation 2.2, and  $\vec{p}_{r_i}$  is the difference in pressurisation acting on the structure, which can be represented as:

$$\vec{p}_{r_i} = P \cdot \vec{A}_{p_i}$$

with

$P$  being the difference in pressure in the internal and external environment, for simplicity considered equal to the internal pressurisation, as the atmospheric pressure on both the Moon and Mars can be negligible, and

$\vec{A}_{p_i} = [A_{yz_i} \ A_{xz_i} \ A_{xy_i}]$  the projected areas in  $yz, xz, xy$  with respect to the adjacent nodes  $a, b, c, d$ . E.g., for node “i” and the grid exemplified in Figure 2.1, the projected area for the first time-step (starting with a flat form) is:

$$\vec{A}_{p_i} = [0 \ 0 \ 1] \quad \text{or}$$

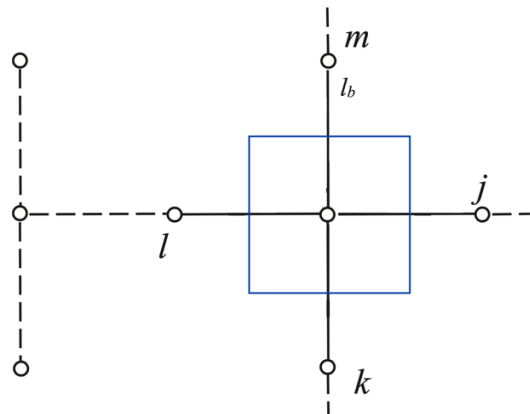
$$A_{yz_i} = \frac{|x_i - x_j|}{2} \cdot \frac{|z_i - z_m|}{2} + \frac{|x_i - x_l|}{2} \cdot \frac{|z_i - z_m|}{2} + \frac{|x_i - x_l|}{2} \cdot \frac{|z_i - y_k|}{2} + \frac{|x_i - x_j|}{2} \cdot \frac{|z_i - z_k|}{2} \quad (\text{Equation 2.12})$$

$$A_{xz_i} = \frac{|x_i - x_j|}{2} \cdot \frac{|z_i - z_m|}{2} + \frac{|x_i - x_l|}{2} \cdot \frac{|z_i - z_m|}{2} + \frac{|x_i - x_l|}{2} \cdot \frac{|z_i - y_k|}{2} + \frac{|x_i - x_j|}{2} \cdot \frac{|z_i - z_k|}{2} \quad (\text{Equation 2.13})$$

$$A_{xy_i} = \frac{|x_i - x_j|}{2} \cdot \frac{|y_i - y_m|}{2} + \frac{|x_i - x_l|}{2} \cdot \frac{|y_i - y_m|}{2} + \frac{|x_i - x_l|}{2} \cdot \frac{|y_i - y_k|}{2} + \frac{|x_i - x_j|}{2} \cdot \frac{|y_i - y_k|}{2} \quad (\text{Equation 2.14})$$

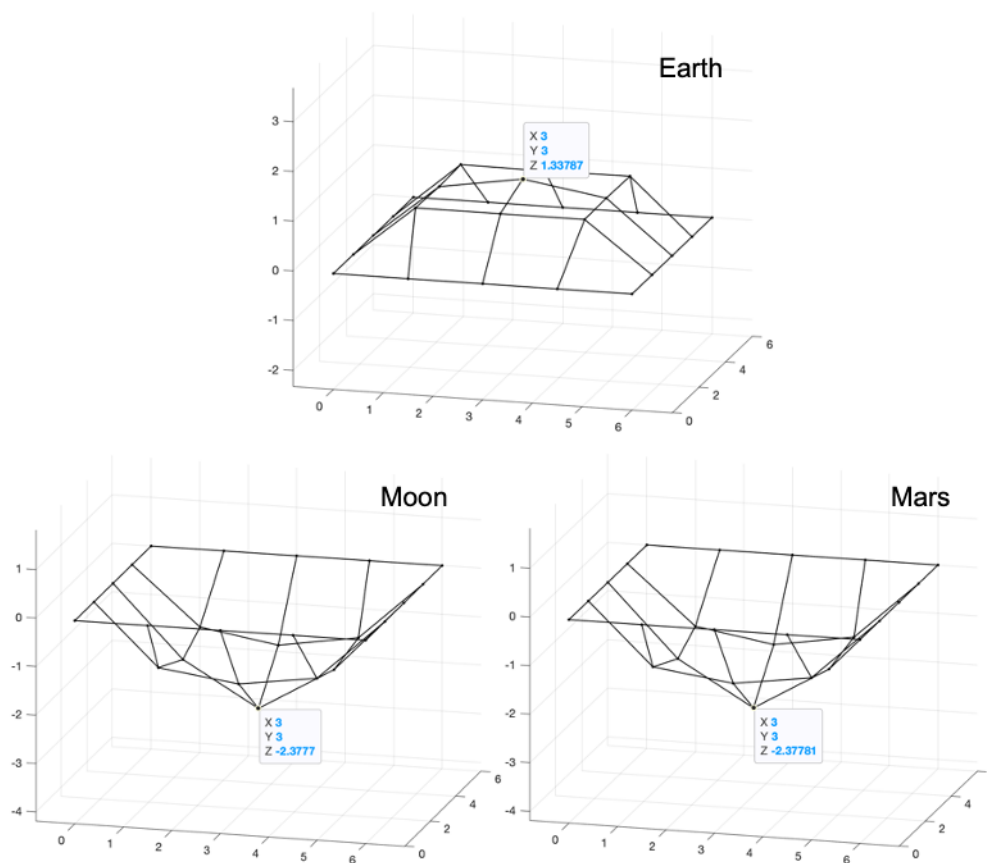
As represented in the figure:

Figure 2.5: projected areas for node “i”



This calculation is repeated for every node and each time step until reaching dynamic equilibrium, with zero velocity and zero acceleration on the nodes, i.e., the coordinates of the node obtained for the final step are the same as those calculated in the previous one. To illustrate the behaviour of three structures on terrestrial, lunar and Martian environment, let us take a simple square grid of 25 nodes, with spacing of  $l = 1.5 \text{ m}$ :

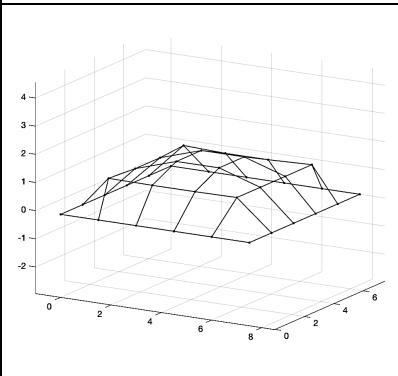
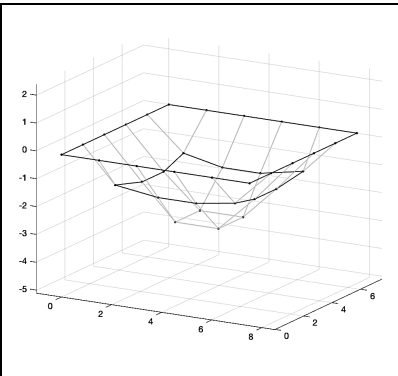
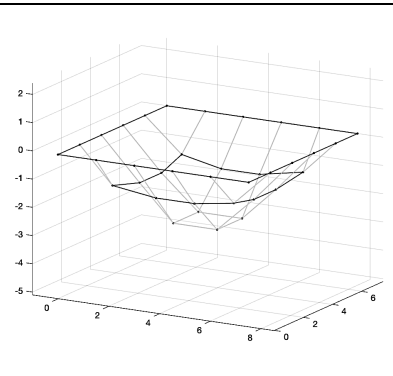
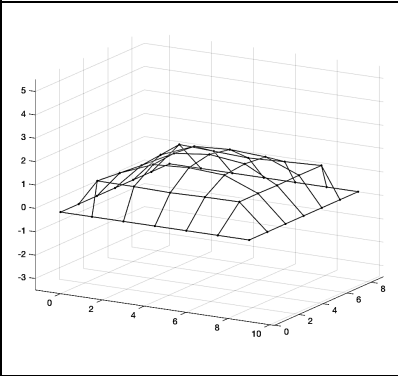
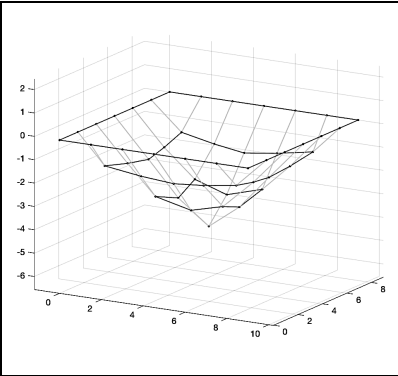
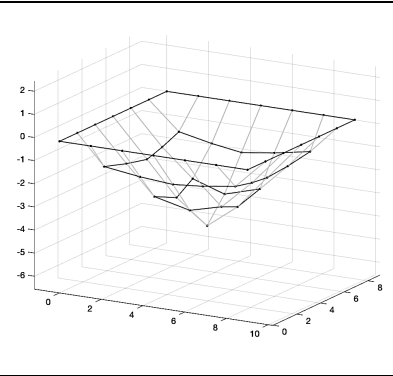
Figure 2.6: 25-node grids on each of the three environments



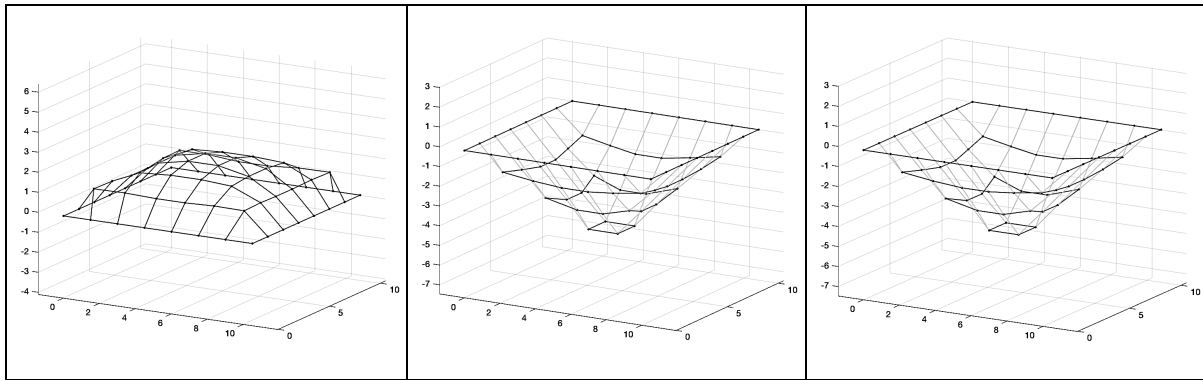
	Earth	Moon	Mars
gravity [ $\text{m/s}^2$ ]	9.81	1.62	3.73
internal pressure [kPa]	0	101.3	101.3
span [m]	6	6	6
$z$ [m]	1.34	- 2.38	- 2.38

Upon initial observation, the prevailing influence of pressure becomes evident. While on Earth the optimised shape resembles a dome, on the Moon and Mars it assumes an inverse configuration. This dominance is further substantiated by the nearly identical minimum values of  $z$  found for both extraterrestrial environments, notwithstanding the gravitational force on Mars being over twice that observed on the Moon. The same comparison can be done for other layouts, also with spacing of  $l = 1.5\text{ m}$ , obtaining the same pattern.

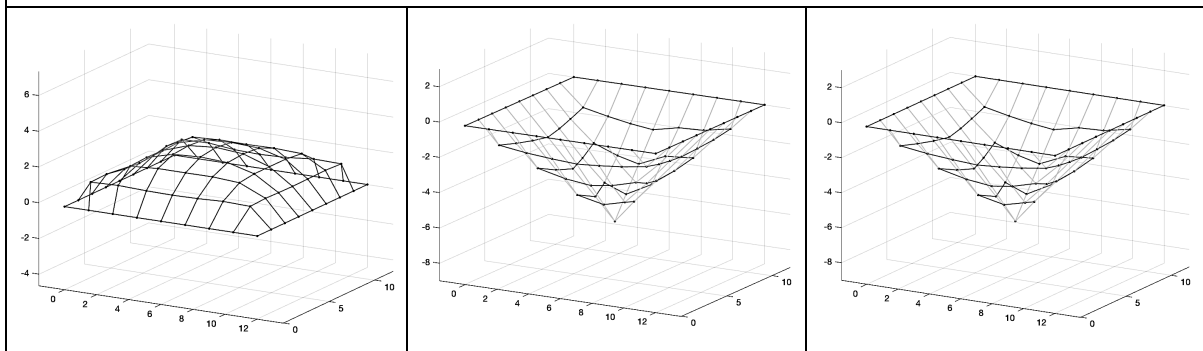
Table 2.2: Different node grids on each of the three environments

Earth	Moon	Mars
$p = 0\text{ kPa}$	$p = 101.3\text{ kPa}$	$p = 101.3\text{ kPa}$
6x6 nodes		
		
7x7 nodes		
		
8x8 nodes		

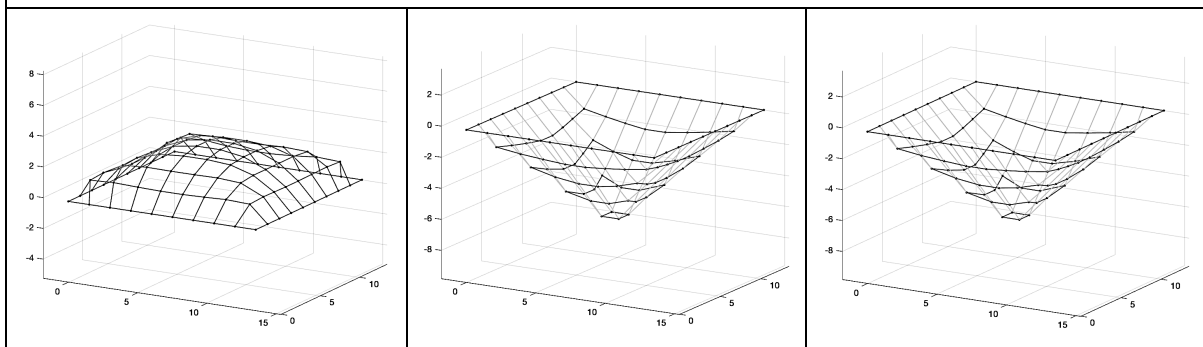




9x9 nodes



10x10 nodes



However, before performing a quantitative analysis, a few comments must be made:

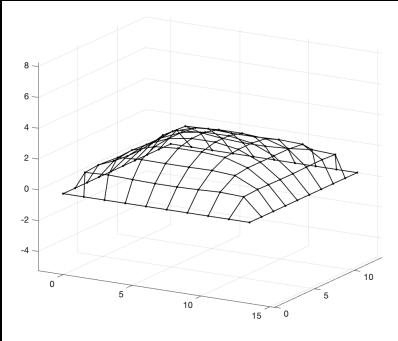
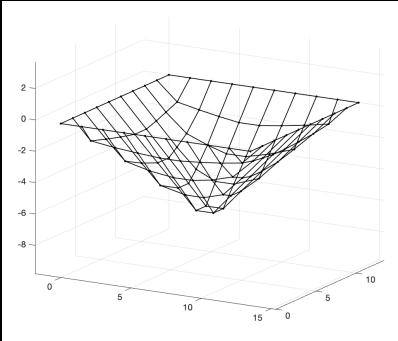
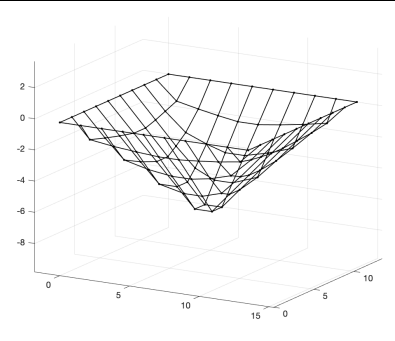
1. The goal of the Multi-Body Rope approach, as well as other form-finding methods, is to obtain an optimised shape for the structure – the method alone does not provide a structural analysis. In no case does this diminish the importance of the obtained results, as they provide valuable information for the conceptual step of a project.
2. The MRA method is designed to obtain a funicular surface, that is, subjected only to axial loads. Consequently, the chosen materials for the construction must be compatible with this characteristic. For a traditional gridshell – on the Earth – the ropes represent beam elements that can be constructed with, e.g., timber or steel.

3. The results provided by the MRA code depend on the input values. Besides the values for gravitational force and internal pressurisation, already mentioned, the analysis depends on a value of mass  $m$  applied for each node and the maximum length  $l_{max}$  that the rope can achieve.

Whereas changes in mass result in little to no change on the final shape and on the maximum/minimum height  $z$ , the maximum length of the rope  $l_{max}$  can lead to considerable changes, especially for smaller grids.

The following comparisons demonstrate these observations, using as base a 10 x 10 grid and spacing  $l = 1.5 m$ .

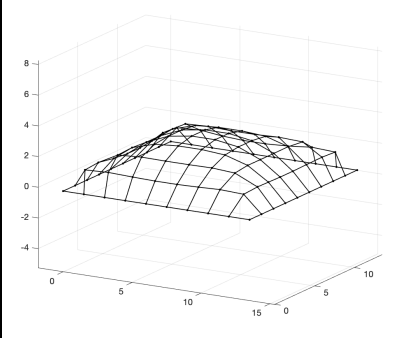
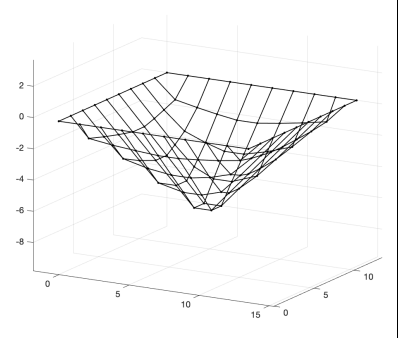
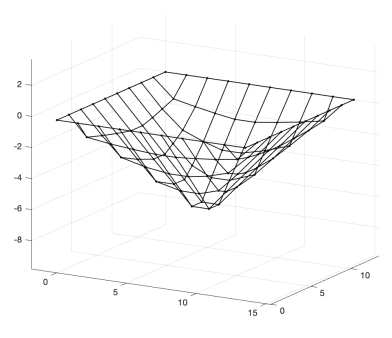
Table 2.3: Impact of different nodal masses

Earth	Moon	Mars
$p = 0 kPa$	$p = 101.3 kPa$	$p = 101.3 kPa$
		
$m = 30 kg, l_{max} = 1.7 m$		
$z_{max} = 3.03$	$z_{min} = -6.14$	$z_{min} = -6.14$
$m = 40 kg, l_{max} = 1.7 m$		
$z_{max} = 2.99$	$z_{min} = -6.14$	$z_{min} = -6.14$
$m = 50 kg, l_{max} = 1.7 m$		
$z_{max} = 2.98$	$z_{min} = -6.14$	$z_{min} = -6.14$

The minimal impact caused by the mass change on the lunar and Martian structures, even smaller than on the terrestrial one, confirms the higher contribution of the internal pressurisation with respect to the gravitational forces in these two environments. Luckily, the results of all structures are barely impacted by the changes of mass, so

an initial estimation of the density of the construction materials is sufficient to obtain an adequate optimised shape, saving one step of the design iterative process.

Table 2.4: Impact of different maximum lengths

Earth	Moon	Mars
$p = 0 \text{ kPa}$	$p = 101.3 \text{ kPa}$	$p = 101.3 \text{ kPa}$
		
$l_{max} = 1.7, m = 30 \text{ kg}$		
$z_{max} = 3.03$	$z_{min} = -6.14$	$z_{min} = -6.14$
$l_{max} = 1.65, m = 30 \text{ kg}$		
$z_{max} = 2.34$	$z_{min} = -6.06$	$z_{min} = -6.06$
$l_{max} = 1.60, m = 30 \text{ kg}$		
$z_{max} = 2.05$	$z_{min} = -5.91$	$z_{min} = -5.91$
$l_{max} = 1.55, m = 30 \text{ kg}$		
$z_{max} = 1.47$	$z_{min} = -5.60$	$z_{min} = -5.60$
$l_{max} = 1.52, m = 30 \text{ kg}$		
$z_{max} = 0.97$	$z_{min} = -5.40$	$z_{min} = -5.40$

Differently than the changes in mass, the changes in maximum length can impact the results for a 10x10 grid. Comparing the structure depth for  $l_{max} = 1.7, m$  and  $l_{max} = 1.52, m$ , there is a reduction of 12%. Once again, the difference is much pronounced in the terrestrial structure, being only subjected to gravitational forces. Also, these

differences are more pronounced for smaller layouts, and may thus be not so significant for larger structures. For example, in a 5x5 grid this reduction is of 28%. Table 2.5 exemplifies this change, considering the structure on Mars ( $g = 3.73 \text{ m/s}^2$ ),  $P = 101.3 \text{ kPa}$  and  $m = 20 \text{ kg}$ .

Table 2.5: Changes in maximum lengths for a 5x5 grid

$l_{max} = 1,7$	$z_{min} = -2,38$
$l_{max} = 1,6$	$z_{min} = -2,05$
$l_{max} = 1,51$	$z_{min} = -1,71$

With a better understanding of the MRA approach, a purposefully analysis can be performed for the lunar and Martian environments.

## CHAPTER 3: ANALYSIS FOR LUNAR AND MARTIAN ENVIRONMENTS

As demonstrated in the previous chapter, there is a significant difference when designing for conditions beyond the Earth, mostly the concomitant action of a lower self-weight – due to lower gravitational forces – and the internal artificial pressurisation that acts mostly against it. On Mars, and by extension also on the Moon, “the required interior pressure is about an order of magnitude greater than the weight of the materials necessary to enclose the space.” [16] Understanding the loads to which a structure must resist is a vital step of the design process, but so is the choice of materials and construction techniques to be applied. This selection can intertwine with two other factors of extreme environments that were mentioned on Chapter 1: large temperature variation and protection against radiation and micro-meteoroids. Aiming at better understanding this strategical side of space design, on overview on the current and future international perspectives will be presented, followed by the hypotheses taken for this work.

### 3.1 TYPES OF STRUCTURES

Considering NASA’s plan of establishing a lunar presence prior to exploring Mars, most international effort is focused on preparing for the Moon, both strategically and in terms of technology development. Hence, it is acceptable to build upon state-of-the-art concepts for lunar bases and extrapolate, when possible, to Mars’ case. One notion that is often discussed is the classification of Lunar Base structures depending on their function and construction type. These are:

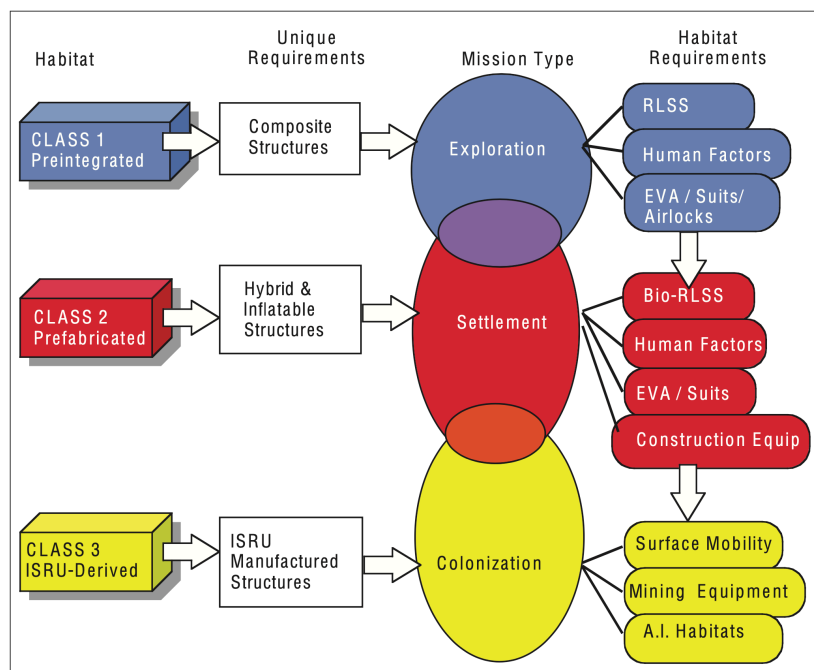
1. Unpressurised structures, used to store equipment and supplies to support lunar missions.
2. Class 1 – pre-integrated structures. Designed and assembled on Earth, these structures are transported on their final shape to be solely installed on the Moon. Generally made of composite materials, adequately resisting the extreme environment. These structures shall provide shelter for the first exploratory missions.

3. Class 2 – prefabricated structures. Mostly hybrid and pneumatic, they are also delivered pre-made. Lightweight during transport and able to provide a great habitable space when deployed, this class of structure is planned for settlement missions. Temperature variation, radiation and micro-meteoroid shielding can be provided by various materials, including regolith, water, and composite materials.
4. Class 3 – structure made of local materials, also known as ISRU-derived. ISRU stands for In-Situ Resources Utilisation and the construction of such structures is a major goal of lunar exploration. Besides limitations on payload, the ability to exploit local resources can expand colonisation capabilities on the Moon and provide valuable insight for ISRU technology on Earth.

Though all classes of surface structures benefit from regolith shielding, for the third class it is viewed as the primary source of protection, as local resources are used for the construction, likely by layered manufacturing. A visualisation of the three classes and their evolutionary path is provided in Figure 3.1.

Another widely discussed perspective is that lunar colonies should be mostly underground structures, taking advantage of natural geologic formations, such as lava tubes, or engineered tunnelling to adequately shield the crew from the extreme conditions of the surface. [17 - 19]

Figure 3.1: Class I, II and III habitats [19]



(RLS = regenerative life support system; EVA = extravehicular activity; A.I. = artificial intelligence)

Comparatively to the Artemis phases, the evolution of habitats also progresses as new missions provide further insight into lunar and Martian environments. Having ISRU-based habitats as the final stage is not by chance, as further information on soil composition is needed and necessary tools are being developed and constantly updated. Due to their lifeless appearances, Moon and Mars may have once been considered barren lands, but with further information on their composition has shown a wealth of raw materials. Moon regolith is primarily composed by four major mineral types: pyroxene, anorthite, olivine, and ilmenite, as well as over 42% of oxygen by mass. Magnesium is considered a candidate ISRU material on the Moon, pervasive in lunar soil, easily cast, used, and recycled. Sulphur-based concrete is also suggested as construction material, given the mineral's availability on lunar soil. Still, processing of regolith may require extensive processing. Martian rocks, composed of silicate minerals, can also be a source of raw materials for construction, e.g., iron and aluminium. Water ice, found in both environments, can be used in the production of conglomerates in situ. [18 - 21]

While the concept of ISRU exists for decades, key technologies with space application are still being developed and constantly improved. These include research on prospective materials, development of mining and extraction tools, and autonomous construction. Though harnessing space resources can significantly reduce the total mass to be launched from Earth, one of the challenges associated with regolith excavation is its extremely fine grained and abrasive nature, raising significant wear concerns. Maximising robotic aid can significantly increase efficiency and crew safety, ideally assuming no necessary human presence to construct and maintain a permanent lunar/Martian outpost. Two products of this ever-evolving research are The All-Terrain Hex-Limbed Extra-Terrestrial Explorer (ATHLETE) and the Planetary Autonomous Construction System (P@X). Both developed by the Jet Propulsion Laboratory of the California Institute of Technology (under a NASA contract), these robotic construction systems can be applied to build and maintain a surface human outpost prior to the crew arrival. Applications of the systems include material delivery (off-loading and transporting large payloads from landers), modular assemble, excavation, tunnel construction, and maintenance. Other performance goals for autonomy and robotics include site preparation, installation of utilities such as power cables, deployment of power plants, and other construction and maintenance activities required for a fully functioning settlement. [22 - 25]

Equally important to the success of the mission is the advance in science materials. Categorised as metals, polymers, ceramics and inorganic glasses and composites, the choice of materials depends on the expected properties depending on the applied

loads and environmental conditions. Material requirements for space application are several, namely high reliability (crew safety); durability, fatigue and corrosion degradation, radiation protection and thermal properties (extreme environment); and lightweight (due to payload restrictions). Although ceramics outperform metals and polymers in terms of thermal properties – melting points, ability to withstand high temperatures, strength, and thermal expansion properties – their brittleness is usually unsatisfactory for structural behaviour. Metals, although of adequate strength, do not perform well under high temperatures. The exploration of composites targets a balanced combination of properties and is very popular for space and aerospace applications, e.g., the use of fibre-reinforced polymer composite materials for the construction of aircrafts and spacecrafts. Common fibers used for aircrafts are glass, aramid, and carbon, aiming at higher strength and moderate modulus. However, not every composite that is adequate for aircraft construction is also suitable for space applications, as in this case high modulus and moderate strength are preferred. [26 - 29]

Other materials largely used for space applications are alloys, in particular Aluminium and Titanium alloys, developed to minimise weight while maintaining comparable strength. For example, aluminium alloys containing lithium are well known for their benefits in reducing density and increasing Young's modulus, proportionally to their Li content, and can be used for structural framing. Besides providing adequate structural resistance, other materials are applied to ensure thermal properties and radiation shielding – polymeric matrices, multi-layer insulation blanketing and aerogels – and visibility – borosilicate glass for windows. [30-33]

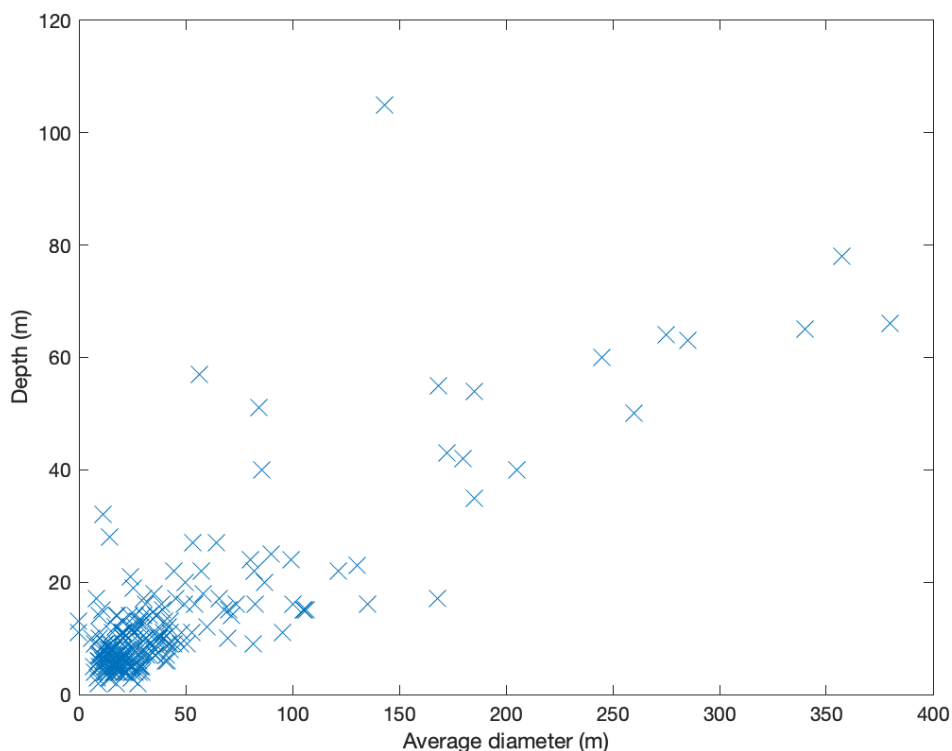
In brief, habitats for space application can be designed in many shapes and materials. The evolution of design choices on the Moon is projected to follow three general phases: (a) support shelters to store scientific equipment; (b) temporary pre-integrated or deployable structures for initial exploration, most of them of spherical, cylindrical and toroid shell shape; and (c) long-term habitats made exploiting in-situ resources. Habitable structures falling under the third category are the furthest to realisation, and the least rigidly defined, but are the ones that can lead to large-scale settlements and colonies. Proof-of-concept is expected to increase building upon the knowledge and technology to be developed with the exploitation of type (a) and (b) shelters, as well as robotic and crewed surface missions. Likely lunar colonies will be composed by a combination of all three types of habitats, as well as hybrids of the categories. For the case of Mars, ISRU-based structures are perhaps the most important due to the extreme distance and consequent payload cost, limiting the resources that can be transported. Autonomous construction is also a key feature, highlighting the



importance of space technology previously mentioned. Future outpost strategies for the Martian surface are even harder to predict as, according to the Global Exploration Map, future Mars missions will take place after the stabilisation of the Artemis Base Camp, leaving much time for scientific development. [3, 17-19]

In parallel, researchers are constantly updating the mapped areas of the lunar and Martian surface, including the localisation and estimated dimensions of lava tubes. The existence of these geological formations and the idea of exploiting them to construct sub-surface outposts was hypothesised prior to their factual discovery. Besides protection from cosmic rays and dust, interiors of lava tubes provide a relatively constant temperature environment, around  $-20^{\circ}\text{C}$ . However, important points to notice are the volume (not too large), orientation and angle of incidence with the surface – can be difficult to enter. [17] Figure 3.2 shows a distribution of lunar pits based on their average diameter and depth, based on data from the Lunar Reconnaissance Orbiter Camera (LROC). [19]

Figure 3.2: Lunar pits (based on LROC)



As observed in the figure, there are plenty of potential pits to be explored as habitats, even considering smaller geometries, around 10 meters of diameter and depth. A few examples, but not exhaustive, are shown in Table 3.1. Other features of the pit can be considered in the choice, such as location (e.g., Artemis Base Camp is planned for the South Pole, near the Shackleton crater) and accessibility, as well as resources on the area, such as water ice and minerals. Analogously to what is observed on Earth, lunar and Martian soil are not homogeneous across their surface. Visual data from orbiters and further examinations from rovers can give input on regolith grain size, chemical composition, and geological formation. Depending on the project goal, on the materials and equipment to be utilised, pits located in one area might be more advantageous depending on its regolith composition.

Table 3.1.: Lunar pits (based on LROC)

Name	funnel maximum diameter [m]	funnel minimum diameter [m]	funnel average diameter [m]	depth [m]
Crookes 5d	6	6	6	10
King 39	8	6	7	5
King 27	9	6	7,5	9
King 8b	8	8	8	17
King 13b	10	8	9	7
King 3b	9	9	9	6
Dollond E 1d	11	8	9,5	14
Messier A 2b	11	8	9,5	10
King 6	10	10	10	7
Lalande 12	11	9	10	11
Messier A 1	13	9	11	15
Dollond E 1c	12	11	11,5	32

In sum, designing a habitat to exploit existing lunar pits can have a few advantages:

1. Radiation safety: “Below a depth of 6 m, simulations show that there are no radiation effects due to, or induced by, galactic cosmic rays (GCRs). Below 1 m, there are no radiation effects due to, or induced by, solar particles events (SPE).” [18]
2. Mild temperature variation – “The interiors of lava tubes provide a relatively constant-temperature environment, estimated at  $-20\text{ }^{\circ}\text{C}$ ” [17] – and potentially less dust, reducing complications such as abrasion. [19]
3. Compatibility with the optimised shape provided by the MRA analysis (designed as a roof for the pit).
4. Possibility of integration with other habitat types, including multi-level designs, depending on pit depth. E.g., an inflatable structure can be inserted on the lava tube, then pressurised, benefiting from the shielding against thermal variation, radiation, and micro-meteoroids. [17]

## 3.2 STRUCTURE PROPOSITION

Considering the mentioned advantages of the lava tubes and the inverse-dome shape proposed by the Multi-Body Rope Approach results, an interesting application of the optimised geometry is the proposition of a roof. The shape and some characteristic values of the MRA result used as basis for the following analysis are shown in Figure 3.3 and Table 3.2.

Figure 3.3: Model geometry

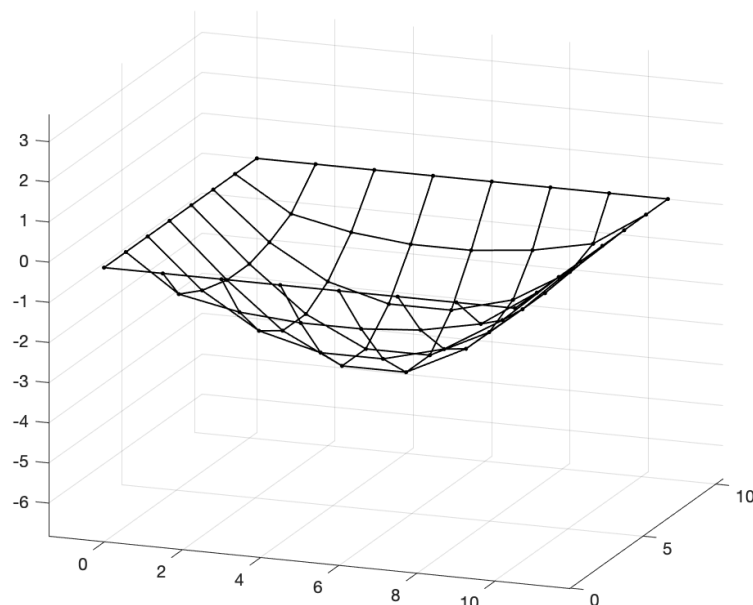


Table 3.2: Model data

Nodes	8x8
Span dimensions	10,5 x 10,5 m <sup>2</sup>
Depth	-3.17 m

As observed in the previous chapter, the geometric differences between the lunar and Martian structures are negligible. The illustrated model is thus representative of both situations. Another important comment is related to the value of internal pressurisation. Aiming at reducing the loads to which the structure is subjected to, especially considering the major role played by pressure, it is possible to assume values lower than 101.3 kPa. “Historical internal pressures used for NASA programs have ranged from 34.5 kPa (5 psi; 21.300 kg/m<sup>2</sup> on the Moon) to 101.4 kPa (14.7 psi; 62.600 kg/m<sup>2</sup>) to provide a liveable environment for the astronauts” [33]. This is an acceptable range because the minimal internal pressure to avoid altitude sickness is of at least 26 to 30 kPa, if composed purely of oxygen. To avoid the fire hazard of pure oxygen and provide a more comfortable environment, a minimum pressure of 51.7 kPa is suggested [34]. For the MRA calculation, a value of 70 kPa was chosen for the internal pressurisation, similarly to the habitats proposed by Ruess, Schaenzlin, and Benaroya (69 kPa) and for the lunar lander pressure vessel (65.5 kPa).

The structural analysis can be performed on the Finite Element Analysis (FEA) software LUSAS ©. Regardless of the program, representative results are bound to the correct definition of geometrical properties, loads, and boundary conditions. On LUSAS ©, input data include: (a) geometry, (b) mesh, (c) section properties, (d) material properties, (e) supports, and (f) loading. The shape illustrated on Figure 3.3 was imported to the FEA software by means of a Grasshopper©-generated .dxf file to be analysed as a surface.

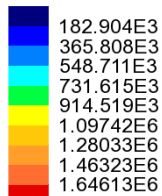
The selection of material properties for the structure is complicated by the limited knowledge of the Lunar and Martian environments, coupled with uncertainties surrounding the production of compression-resistant materials utilizing in-situ resources. The simplest material demonstrating significant compression resistance is a brick. Considering constraints in energy consumption and material availability on both the Moon and Mars, it is likely that only a highly porous brick can be feasibly obtained. Literature on porous materials [35-37] indicates that highly porous materials

exhibit a Young's modulus significantly lower than the theoretical value, typically around 20-30% of the fully dense equivalent. Given the typical Young's modulus values for commercial bricks on Earth, ranging from 15-20 GPa [38], a reasonable estimate for the Young's modulus in this context is 5 GPa. Regarding density, starting from a full density of 2600-3000 kg/m<sup>3</sup>, a conservative choice would be 1800 kg/m<sup>3</sup>. For such a brittle material, the Poisson's ratio is expected to fall within the range of 0.2-0.3, with a reasonable assumption placed at approximately 0.25. Also considering a standard brick size, the appointed thickness is 20 centimetres.

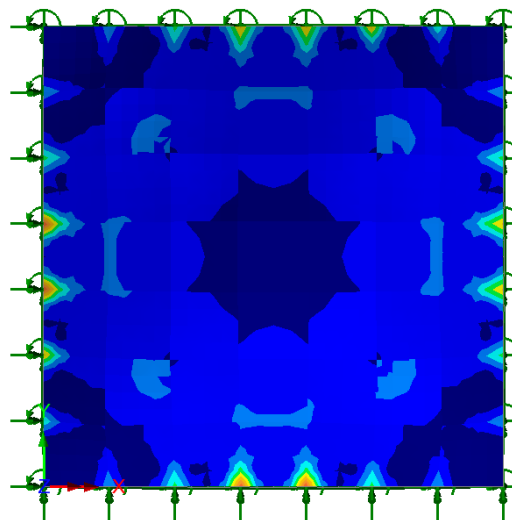
Fixed for both translation and rotation, the structure is subjected to 3 load scenarios – gravity on the Moon (1), gravity on Mars (2) and internal pressure (3) – and 2 combinations – (1+3) and (2+3). The loading scenarios are shown in Figures 3.4 to 3.6, and the obtained results in Figures 3.7 to 3.14. Although not identical, the results for the lunar and the Martian environment are similar, as expected.

Figure 3.7

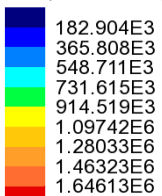
Combination Moon  
Entity: Force/Moment - Thick Shell  
Component: NE (Units: N/m)



Maximum 1.65543E6 at node 742  
Minimum 9.29403E3 at node 729



Combination Moon  
Entity: Force/Moment - Thick Shell  
Component: NE (Units: N/m)



Maximum 1.65543E6 at node 742  
Minimum 9.29403E3 at node 729

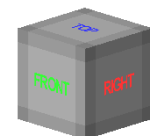
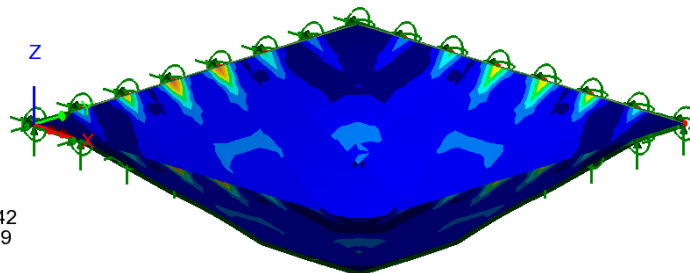
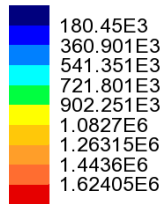
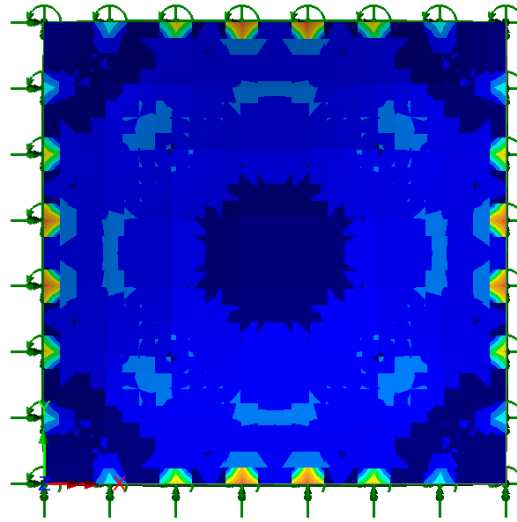


Figure 3.8

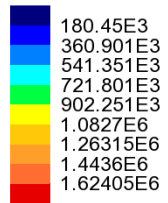
Combination Mars  
 Entity: Force/Moment - Thick Shell  
 Component: NE (Units: N/m)



Maximum 1.63274E6 at node 742 of element 673  
 Minimum 8.69224E3 at node 726 of element 739



Combination Mars  
 Entity: Force/Moment - Thick Shell  
 Component: NE (Units: N/m)



Maximum 1.63274E6 at node 742 of element 673  
 Minimum 8.69224E3 at node 726 of element 739

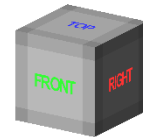
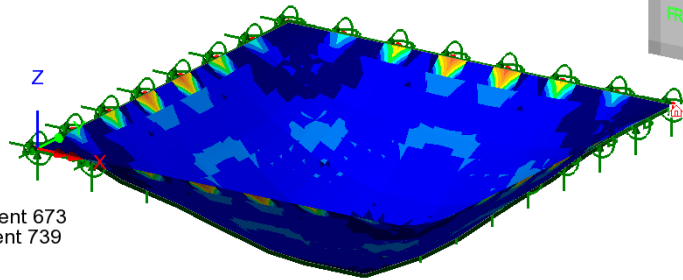
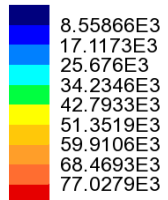
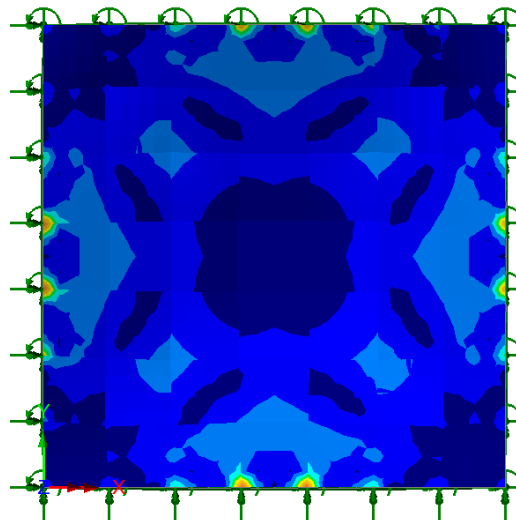


Figure 3.9

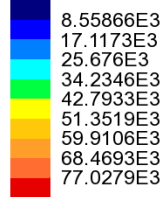
Combination Moon  
 Entity: Force/Moment - Thick Shell  
 Component: ME (Units: N.m/m)



Maximum 78.4268E3 at node 742  
 Minimum 1.39891E3 at node 9



Combination Moon  
 Entity: Force/Moment - Thick Shell  
 Component: ME (Units: N.m/m)



Maximum 78.4268E3 at node 742  
 Minimum 1.39891E3 at node 9

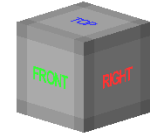
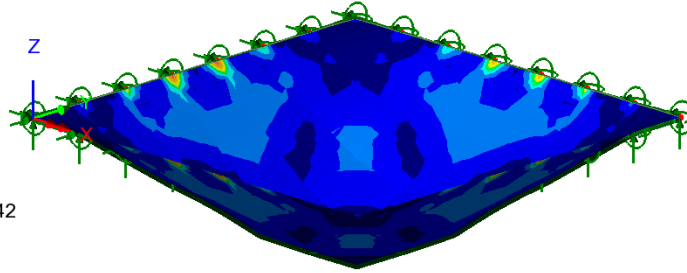
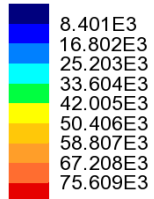
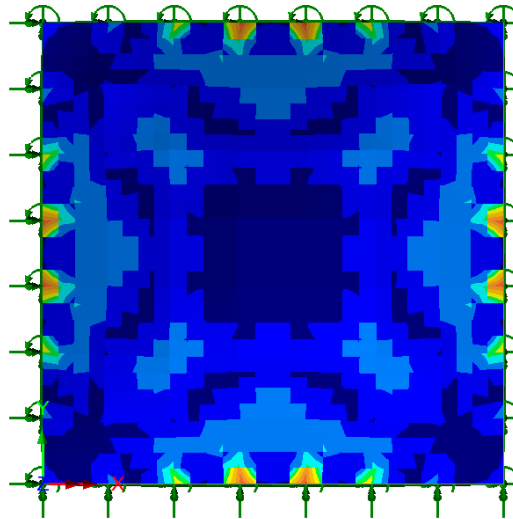


Figure 3.10

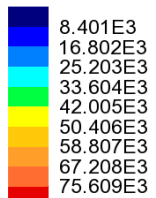
Combination Mars  
 Entity: Force/Moment - Thick Shell  
 Component: ME (Units: N.m/m)



Maximum 77.809E3 at node 742 of element 673  
 Minimum 2.20004E3 at node 7 of element 6



Combination Mars  
 Entity: Force/Moment - Thick Shell  
 Component: ME (Units: N.m/m)



Maximum 77.809E3 at node 742 of element 673  
 Minimum 2.20004E3 at node 7 of element 6

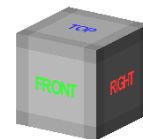
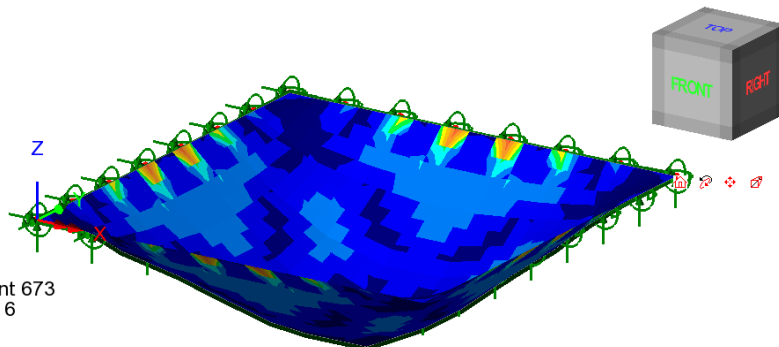
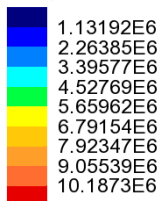
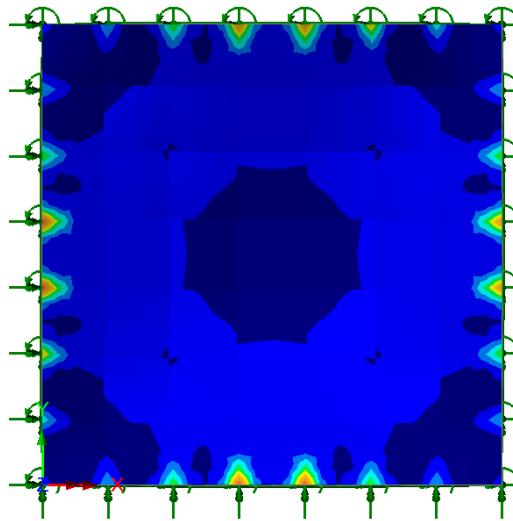


Figure 3.11

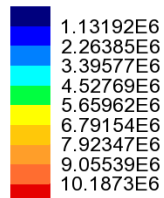
Combination Moon  
 Entity: Stress (middle) - Thick Shell  
 Component: SE (Units: N/m<sup>2</sup>)



Maximum 10.2632E6 at node 742  
 Minimum 75.8909E3 at node 727



Combination Moon  
 Entity: Stress (middle) - Thick Shell  
 Component: SE (Units: N/m<sup>2</sup>)



Maximum 10.2632E6 at node 742  
 Minimum 75.8909E3 at node 727

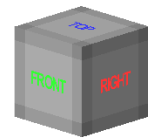
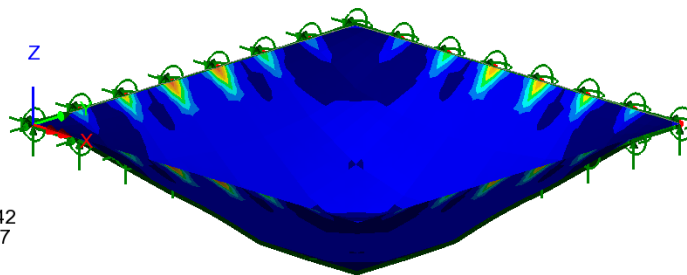
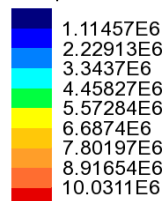
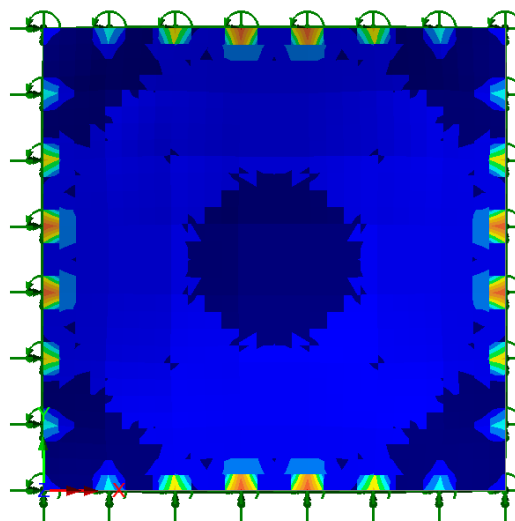


Figure 3.12

Combination Mars  
 Entity: Stress (middle) - Thick Shell  
 Component: SE (Units: N/m<sup>2</sup>)

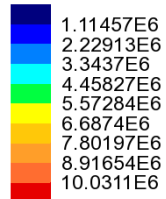


Maximum 10.1472E6 at node 742 of element 689  
 Minimum 116.072E3 at node 727 of element 782





Combination Mars  
 Entity: Stress (middle) - Thick Shell  
 Component: SE (Units: N/m<sup>2</sup>)



Maximum 10.1472E6 at node 742 of element 689  
 Minimum 116.072E3 at node 727 of element 782

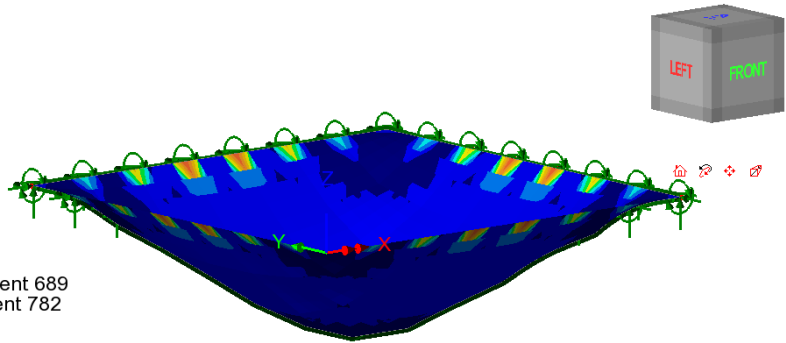
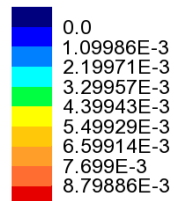
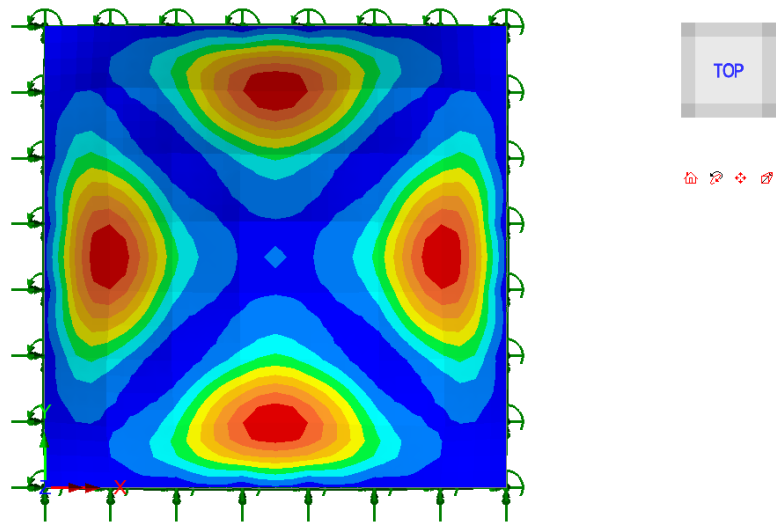


Figure 3.13

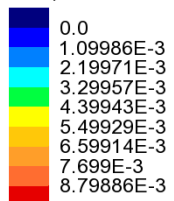
Combination Moon  
 Entity: Displacement  
 Component: RSLT (Units: m)



Maximum 9.89871E-3 at node 352  
 Minimum 0.0 at node 730



Combination Moon  
 Entity: Displacement  
 Component: RSLT (Units: m)



Maximum 9.89871E-3 at node 352  
 Minimum 0.0 at node 730

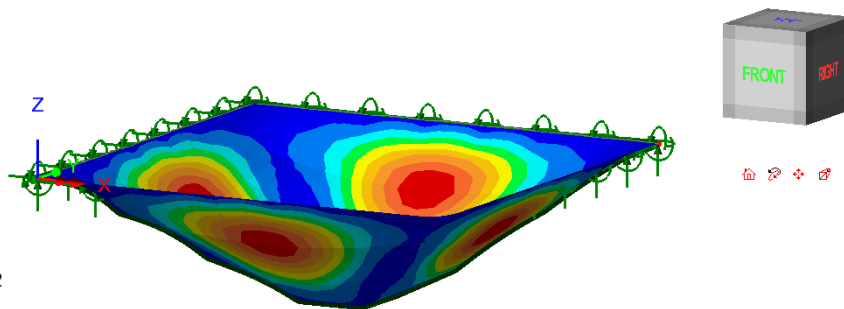
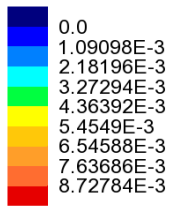
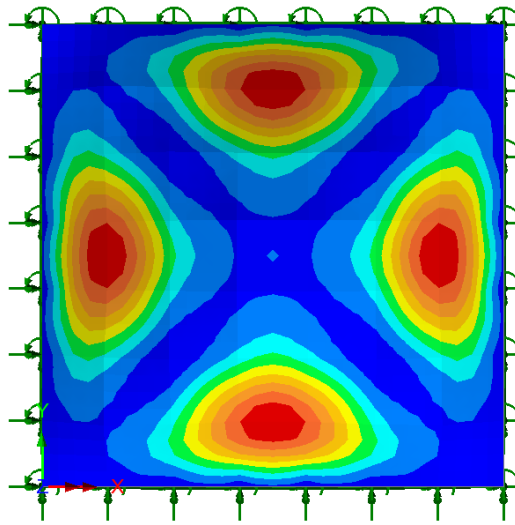


Figure 3.14

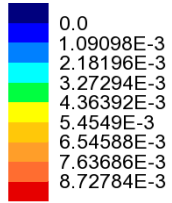
Combination Mars  
Entity: Displacement  
Component: RSLT (Units: m)



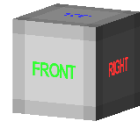
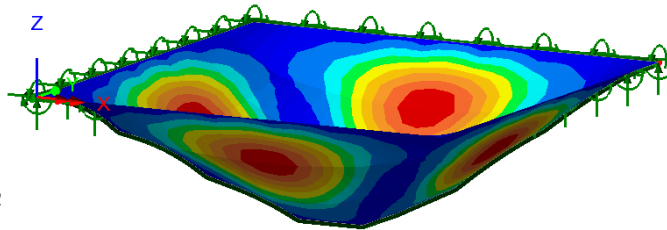
Maximum 9.81882E-3 at node 352  
Minimum 0.0 at node 730



Combination Mars  
Entity: Displacement  
Component: RSLT (Units: m)



Maximum 9.81882E-3 at node 352  
Minimum 0.0 at node 730



## CONCLUSION

This thesis sought to contribute to the existing development of habitat structures for lunar and Martian surfaces, understanding their behaviour with respect to the applied loads and mostly the differences in design assumptions when compared to terrestrial constructions. The findings show that the major player is the internal pressurisation, essential to sustain human life outside of the Earth, both for obtaining the optimal shape and for the structural analysis. Constructability is supported by state-of-the-art research on lunar pits, chosen as basis for the habitat construction, in which the dimensioned element was the roof – exploiting the natural geological formation at its fullest. Moreover, current development of construction equipment for space application and materials science support the use of minerals found on lunar and Martian soil as base for ISRU-based construction materials. Exploitation of in situ resources is a key target of space exploration, facilitating future colonisation by minimising the required payload. Additionally, the use of in situ resources can assure radiation shielding, especially inside of lava tubes, which also facilitate thermal control and reduce dust exposition. Finally, the study of a topic of low technology readiness poses several limitations, but presents the opportunity to contribute to an ever-evolving field of research such as space exploration.

## REFERENCES

- [1] "Exploring Space". Science Museum, London, UK.
- [2] Smith, M., Craig, D., Herrmann, N., Mahoney, E., Krezel, J., McIntyre, N., & Goodliff, K. (2020, March). The artemis program: An overview of nasa's activities to return humans to the moon. In 2020 IEEE Aerospace Conference (pp. 1-10). IEEE.
- [3] Landgraf, M., Reynolds, J., Sato, N., Goodliff, K., Esty, C., & Picard, M. (2021, October). Lunar surface concept of operations for the global exploration roadmap lunar surface exploration scenario. In 72nd International Astronautical Congress 2021 (No. IAC-21, A5, 1, 5, x66702).
- [4] Nair, G. M., Murthi, K. S., & Prasad, M. Y. S. (2008). Strategic, technological and ethical aspects of establishing colonies on Moon and Mars. *Acta astronautica*, 63(11-12), 1337-1342.
- [5] Beatty, J. K., Petersen, C. C., & Chaikin, A. (Eds.). (1999). *The new solar system*. Cambridge University Press.
- [6] "Our Solar System". Adler Planetarium, Chicago, USA.
- [7] The Moon – NASA website .  
<https://nssdc.gsfc.nasa.gov/planetary/planets/moonpage.html>
- [8] Reneau, A. (2020). *Moon First and Mars Second: A Practical Approach to Human Space Exploration*. Springer Nature.
- [9] Schrunk, D. G. (2002). The Moon: Optimum location for the first industrial/scientific base in space. In *Space 2002 and Robotics 2002* (pp. 122-128).
- [10] Planetary Fact Sheet, Moon Fact Sheet, Mars Fact Sheet – NASA website.  
<https://nssdc.gsfc.nasa.gov/planetary/factsheet/index.html>
- [11] Technology Readiness Levels – NASA website.  
<https://www.nasa.gov/directorates/somd/space-communications-navigation-program/technology-readiness-levels/>
- [12] Gaudenzi, P. (n.d.). Design criteria and procedures of space structures. Universita di Roma / European Space Agency.  
[http://dma.ing.uniroma1.it/users/ls\\_sas/MATERIALE/Design%20criteria%20and%20procedures%20of%20space%20structures.pdf](http://dma.ing.uniroma1.it/users/ls_sas/MATERIALE/Design%20criteria%20and%20procedures%20of%20space%20structures.pdf)
- [13] Manuello Bertetto, A., Melchiorre, J., Sardone, L., & Marano, G. C. (2022). MULTI-BODY ROPE APPROACH FOR THE FORM-FINDING OF SHAPE OPTIMIZED GRID

SHELL STRUCTURES. In Pursuing the Infinite Potential of Computational Mechanics. International Centre for Numerical Methods in Engineering, CIMNE.

[14] Manuello, A. (2020). Multi-body rope approach for grid shells: form-finding and imperfection sensitivity. *Engineering Structures*, 221, 111029.

[15] Carpinteri, A. (2017). *Advanced structural mechanics*. CRC Press.

[16] Petrov, G., & Ochsendorf, J. (2005). Building on mars. *Civil Engineering Magazine Archive*, 75(10), 46-53.

[17] Cohen, M. M., & Benaroya, H. (2009). Lunar-base structures. *Out of This World: The New Field of Space Architecture*, 179-204.

[18] Benaroya, H. (2017). Lunar habitats: A brief overview of issues and concepts. *Reach*, 7, 14-33.

[19] Jablonski, A. M., & Ogden, K. A. (2008). Technical requirements for lunar structures. *Journal of Aerospace Engineering*, 21(2), 72-90.

[20] Spudis, P. D. (2003). Harvest the Moon. *Astronomy*, 31(6), 42-47.

[21] Sanders, G. B., & Larson, W. E. (2013). Progress made in lunar in situ resource utilization under NASA's exploration technology and development program. *Journal of Aerospace Engineering*, 26(1), 5-17.

[22] Zacny, K., Voecks, G., Vendiola, V., Smith, M., Sims, M., Sherwood, B., ... & Howe, A. S. (2019). Planetary Autonomous Construction System (P@ X).

[23] Howe, A. S., Wilcox, B., Barmatz, M., & Voecks, G. (2016, April). ATHLETE as a mobile ISRU and regolith construction platform. In *15th Biennial ASCE Conference on Engineering, Science, Construction, and Operations in Challenging Environments* (pp. 560-575). Reston, VA: American Society of Civil Engineers.

[24] Yashar, M., Ciardullo, C., Morris, M., Pailles-Friedman, R., Moses, R., & Case, D. (2019, July). Mars x-house: Design principles for an autonomously 3D-printed ISRU surface habitat. *49th International Conference on Environmental Systems*.

[25] Okushi, J. (1996). First Mars Outpost Architectural Study. In *Engineering, Construction, and Operations in Space V* (pp. 928-934).

[26] Williams, J. C., & Starke Jr, E. A. (2003). Progress in structural materials for aerospace systems. *Acta materialia*, 51(19), 5775-5799. [26] Composite materials for aerospace applications (Mangalgiri, 1999)

[27] Nayak, N. V. (2014). Composite materials in aerospace applications. *International Journal of Scientific and Research Publications*, 4(9), 1-10.

- [28] Williams, J. C., & Starke Jr, E. A. (2003). Progress in structural materials for aerospace systems. *Acta materialia*, 51(19), 5775-5799.
- [29] Yin, P. K. (1989). A preliminary design of interior structure and foundation of an inflatable lunar habitat. Texas A&M Univ., NASA (ASEE Summer Faculty Fellowship Program, 1989, Volume 2. [30] Aluminum-Copper-Lithium Alloy 2050 Developed for Medium to Thick Plate – ph. Lequeu
- [31] Bheekhun, N., Talib, A., Rahim, A., & Hassan, M. R. (2013). Aerogels in aerospace: an overview. *Advances in Materials Science and Engineering*, 2013.
- [32] Tsuyuki, G., Birur, G., Novak, K., & Stultz, J. (2001, January). Lightweight thermal insulation for Mars surface applications. In *39th Aerospace Sciences Meeting and Exhibit* (p. 213).
- [33] Ruess, F., Schaenzlin, J., & Benaroya, H. (2006). Structural design of a lunar habitat. *Journal of Aerospace Engineering*, 19(3), 133-157.
- [34] Belvin, W., Watson, J., & Singhal, S. (2006). Structural concepts and materials for lunar exploration habitats. In *Space 2006* (p. 7338).
- [35] Phani, K. K., & Niyogi, S. K. (1987). Young's modulus of porous brittle solids. *Journal of materials science*, 22, 257-263.
- [36] Kováčik, J. (1999). Correlation between Young's modulus and porosity in porous materials. *Journal of materials science letters*, 18(13), 1007-1010.
- [37] Choren, J. A., Heinrich, S. M., & Silver-Thorn, M. B. (2013). Young's modulus and volume porosity relationships for additive manufacturing applications. *Journal of materials science*, 48, 5103-5112.
- [38] Makoond, N., Pela, L., & Molins, C. (2019). Dynamic elastic properties of brick masonry constituents. *Construction and Building Materials*, 199, 756-770.